New Energy Materials and Devices
https://www.sciltp.com/journals/nemd



Review

Check for updates

Advances in Graphite-Based Dual-Ion Batteries toward Sustainable Energy Applications

Hanwen Zhang [1], Faiza Arshad [2], Areeba Kaleem [3], Xianglin Xiang [4], Liqianyun Xu [1,*], Renjie Chen [5,6] and Li Li [5,6,*]

[1] National and Local Joint Engineering Research Center for LIBs and Materials Preparation Technology, Key Laboratory of Advanced Battery Materials of Yunnan Province, School of Metallurgical and Energy Engineering, Kunming University of Science and Technology, Kunming 650093, China
[2] School of Chemistry and Chemical Engineering, Beijing Institute of Technology, Beijing 102488, China
[3] Department of Chemistry, Government College University Lahore, Lahore 54000, Pakistan
[4] Faculty of Materials Science and Engineering, Kunming University of Science and Technology, Kunming 650093, China
[5] Beijing Key Laboratory of Environmental Science and Engineering, School of Materials Science and Engineering, Beijing Institute of Technology, Beijing 100081, China
[6] Collaborative Innovation Center of Electric Vehicles in Beijing, Beijing 100081, China
* Correspondence: xuliqianyun@163.com (L.X.); lily863@bit.edu.cn (L.L.)

How To Cite: Zhang, H.; Arshad, F.; Kaleem, A.; et al. Advances in Graphite-Based Dual-Ion Batteries toward Sustainable Energy Applications. *New Energy Materials and Devices* **2026**, *1*(1), 111–140. https://doi.org/10.53941/nemd.2026.100007

Received: 15 September 2026
Revised: 12 October 2026
Accepted: 26 October 2026
Published: 6 November 2026

Abstract: The review examines graphite-based dual-ion batteries extensively, covering the basic working principles of this battery technology, the chemistry of anion and cation intercalation into graphite, charge carriers and electrolytes, and the current limitations and improvement strategies for their progress. We begin by reviewing the fundamental intercalation chemistry that has guided decades of research and clarify the different working mechanisms of dual-ion batteries compared with conventional LIBs. The main focus is on the chemistry of graphite intercalation and a detailed analysis of the mechanisms of anionic and cationic charge storage in graphite electrodes. The electrolyte compositions are particularly emphasised, as regards their critical role in the performance of the battery. Then the review systematically summarises the current limitations and corresponding optimisation strategies, including the design of electrode materials, the interphase stabilisation strategies and advanced electrolyte engineering. Finally, we discuss key challenges and suggest potential future research directions to improve high-performance DIB systems for practical energy storage applications. This work will be of interest and practical use to researchers engaged in the development of next generation batteries.

Keywords: dual-ion batteries; graphite; intercalation chemistry; anionic/cationic charge carriers; material innovation

1. Introduction

The global energy transition heavily relies on the development of high-performance EES systems as the basis for energy harvesting, storage, distribution, and utilisation [1–4]. Lithium-ion batteries (LIBs) have been widely used in electronic devices, electric vehicles and other applications since their market introduction in 1991 due to high energy density, long cycle life and no memory effect [5–7]. However, lithium resources are limited and geographically unevenly distributed, which poses challenges for LIBs. The limited availability and increasing price of lithium resources constrain the large-scale energy-storage applications of LIBs, stimulating the urgent development of alternative low-cost rechargeable battery technologies [8,9]. Achieving full carbon neutrality requires the development of next-generation electrical energy systems that are safe, environmentally sustainable,

Copyright: © 2026 by the authors. This is an open access article under the terms and conditions of the Creative Commons Attribution (CC BY) license (https://creativecommons.org/licenses/by/4.0/).
Publisher's Note: Scilight stays neutral with regard to jurisdictional claims in published maps and institutional affiliations.

cost-effective, have high power and energy densities, and are recyclable. Post-lithium batteries are especially promising for stationary storage applications where energy density constraints are relaxed. Batteries based on beyond-lithium cations have recently received much attention as potential alternatives in the area of energy storage research, due to their advantages over traditional lithium-based systems. This has created a lot of research interest in EES systems. In particular, metal-ion batteries including sodium-ion, potassium-ion, dual-ion, and lithium-sulfur batteries, have been potential candidates due to their excellent electrochemical performance and environmental compatibility [10]. Among the emerging EES technologies, DIBs are prominent because the synergistic electrochemical reactions at both electrodes can improve the overall reaction efficiency. DIBs involve the desolvation of ions during discharge that may promote improved low temperature performance, compared with systems based solely on anions or cations [11]. Among these, aluminum–graphite DIBs are especially attractive because of the low cost, abundant electrode materials (natural graphite and aluminium), and excellent cycling stability (>500,000 cycles) [12]. Furthermore, their ultrahigh power density (~95 kW kg^{-1} graphite) allows for fast grid frequency regulation, making them especially suitable for large-scale energy storage applications.

Figure 1a depicts the astonishing geographic concentration of the worldwide refined graphite output, with China accounting for the overwhelming bulk of the global graphite refining capacity. Alongside graphite, major battery minerals such as lithium, cobalt and manganese also display high reliance on a single primary producer, while nickel and rare earths show relatively diversified supply patterns. Between 2023 and 2025, nearly all growth in refined graphite supply came from this leading producer, reflecting the entrenched concentration of the graphite processing industry. Coupled with the downstream economic risks shown in Figure 1b, full graphite export controls would expose more than USD 300 billion of annual overseas production across electric vehicles, battery storage and battery manufacturing sectors. These supply-chain features demonstrate that the raw material availability of graphite constitutes a critical practical constraint for graphite-based dual-ion batteries. Therefore, analysis of graphite supply concentration and trade risks is essential to evaluate the scalability and commercial prospects of graphite-based dual-ion batteries (GDIBs), rather than irrelevant background information. It also reveals the evolutionary trends of research hot spots regarding DIBs and graphite along with the bibliometric statistics from the Web of Science database (Figure 1c,d). Statistics show China has rich graphite resources and a mature battery industry base. In recent years, the research on DIBs has made rapid progress and the research on graphite has kept a stable upward trend in the long-term, which can provide solid resource reserves and theoretical support for the development of dual-ion batteries.

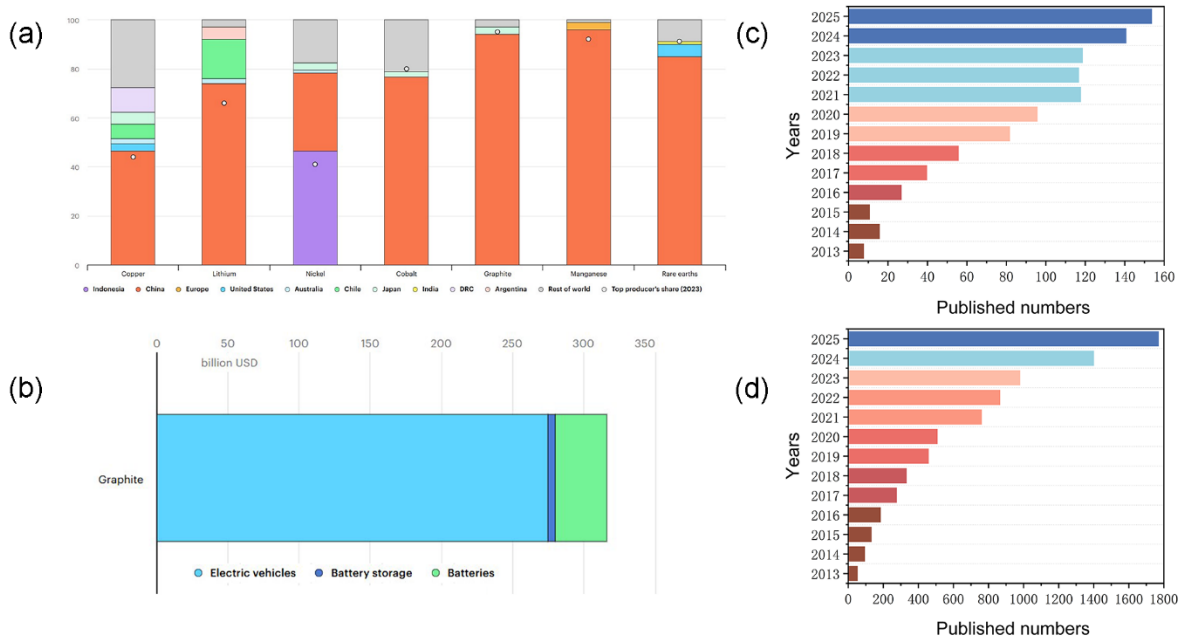


Figure 1. (**a**,**b**) Graphite-related data from "Global Critical Minerals Outlook 2026": (**a**) Country-wise share of refined material production for key battery minerals in 2023 and projected 2025, with the marked proportion denoting the top producer's market share; (**b**) Economic value of downstream production at risk from full graphite export controls in 2025, split by sector (electric vehicles, battery storage, and battery manufacturing, unit: billion USD) (Adapted from ref. [13] under the Creative Commons Attribution 4.0 International License (CC BY 4.0)). (**c**,**d**) Relevant papers retrieved from Web of Science: (**c**) Number of DIB-related publications, 2013–2025; (**d**) Number of graphite-relevant publications, 2013–2025.

The development of DIBs traces back to foundational discoveries concerning anionic intercalation processes in graphite (Figure 2). In 1938, Rüdorff and Hofmann first observed the intercalation of HSO_4^- anions into graphite, leading to the proposed "staging" model in 1940. The model described the layered insertion of ions into graphite cathodes; however, it simplified the complex intercalation phenomena later refined by Daumas and Herold in 1969, who introduced a more realistic model involving simultaneous ion insertion and lattice deformation [14]. This conceptual basis was developed further by early practical demonstrations such as the first dual-graphite cell based on cation and anion intercalation in a non-aqueous electrolyte described in a patent by McCullough and co-workers [15]. Evolution of electrolyte chemistry was also critical, with studies in the 1990s exploring ionic liquids with different cations and anions to enhance electrolyte stability, and in 2000, Dahn et al. utilised *in situ* XRD to elucidate $PF6^-$ intercalation mechanisms into graphite, showing staged intercalation phases [16]. The formal notion of a "dual-ion battery" was proposed by Winter et al. in 2012, inspiring large research efforts to exploit the coupling of cation and anion intercalation for energy storage. These include reversible dual-graphite batteries, electrolyte modification for improved stability and reversibility [17]. In the past few years, research groups led by Tang and Chen have achieved substantial progress in the development of potassium-ion and sodium-ion systems (KDIBs and SDIBs) and holistic battery designs, respectively, focusing on the strategy to solve ion-desolvation issues [18–20]. Then the research focus was changed to develop aqueous/non-aqueous hybrid systems, tailored electrolytes and advanced electrode materials to improve safety, sustainability and performance [21]. Prominent examples are novel modifications of the electrolyte by Yu et al. and high-performance electrode architectures by Xu et al [22,23]. DIB technology has made progress in recent years, but is still behind the LIB technology and in its early development.

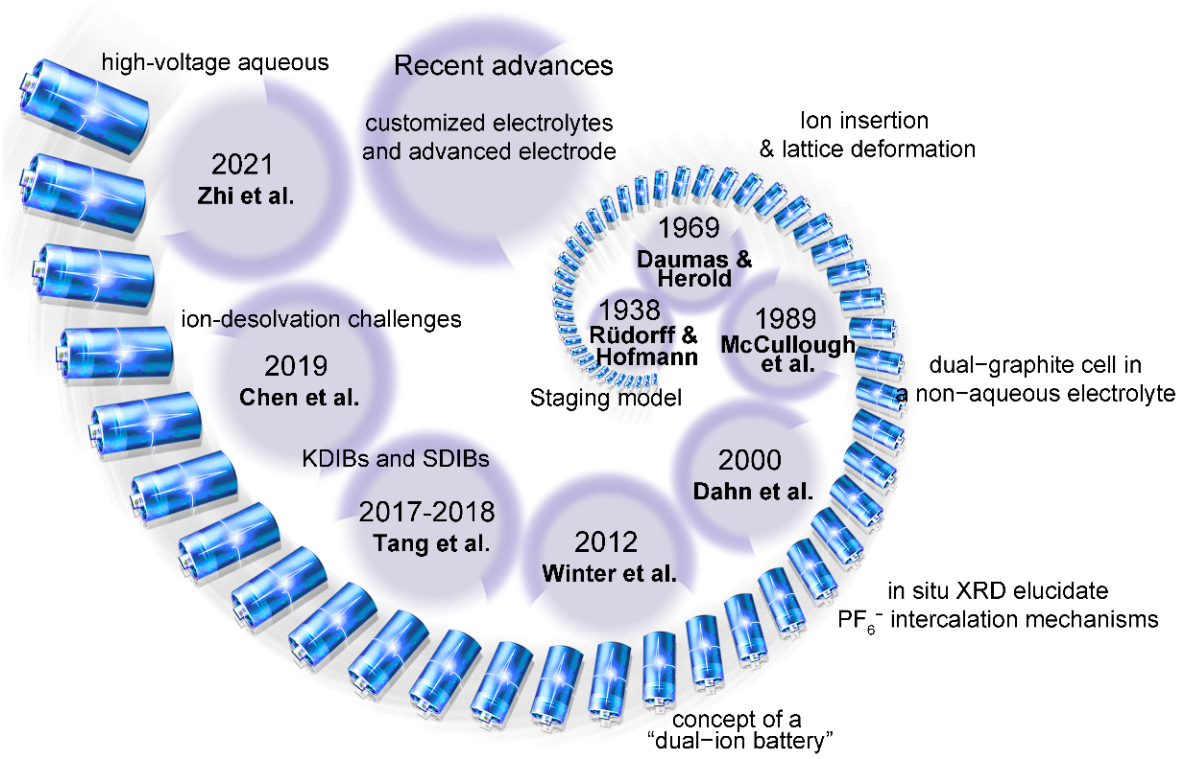


Figure 2. The progress of dual-ion batteries from 1938 until present [14–23].

The anion intercalation into host materials such as graphite and graphite intercalation compounds (GICs) has been explored for many decades [24–27]. These techniques are the basis of current developments in the production of DIBs [28]. Several recent reviews have been published, providing in depth evaluations of DIBs and describing the progress made thus far. In this research, we first clarify the working mechanics of DIBs and emphasise their unique charge storage features by contrast with ordinary LIBs (Section 2). The main topic is devoted to the chemistry of graphite intercalation (Section 3) and deals in particular with the anionic and cationic charge carriers in graphite electrodes (Section 4). Special emphasis is made on electrolyte formulations and their vital function in DIB performance (Section 5). The paper then offers an in-depth examination of the present constraints and the accompanying optimisation options including graphite electrode design, interphase stabilisation approaches and advanced electrolyte engineering (Section 6). Finally, we discuss some of the important obstacles and future

research areas to further develop the GDIBs technology for practical energy storage applications. The structured study offers researchers essential insights and practical help on the design of high-performance DIB systems.

2. Working Principles of Dual-Ion Batteries

During charge/discharge cycles, lithium ions shuttle between the host electrodes, giving rise to the characteristic 'rocking chair' mechanism of LIBs. Unlike traditional "rocking-chair" LIBs, DIBs operate through a distinct mechanism that entails the concurrent storage of both cations and anions within the anode and cathode materials [29]. Ion storage and release in DIBs involve Faradaic reactions such as intercalation, alloying, or deposition, primarily on the anode side for cation storage. As schematically illustrated in Figure 3a, when graphite is used as both the anode and cathode, cations (e.g., Li^+, Na^+, K^+, Ca^{2+}, Al^{3+}, and ionic liquid-based cations) and anions (e.g., PF_6^-, FSI^-, $FTFSI^-$, $TFSI^-$, BF_4^-, $BETI^-$, ClO_4^-, and $DFOB^-$) are simultaneously intercalated/deintercalated into/from the graphite anode and cathode, respectively [30–32]. During discharge, anions and cations move from the cathode and anode into the electrolyte; during charging, they return to their respective electrodes. Since the electrolyte supplies the ionic charge carriers, it should be regarded as an integral component of the active material. Reactions at the cathode and anode during charging of a typical DIB with graphite electrodes involve Li^+ cations and PF_6^- anions as charge carriers [33,34].

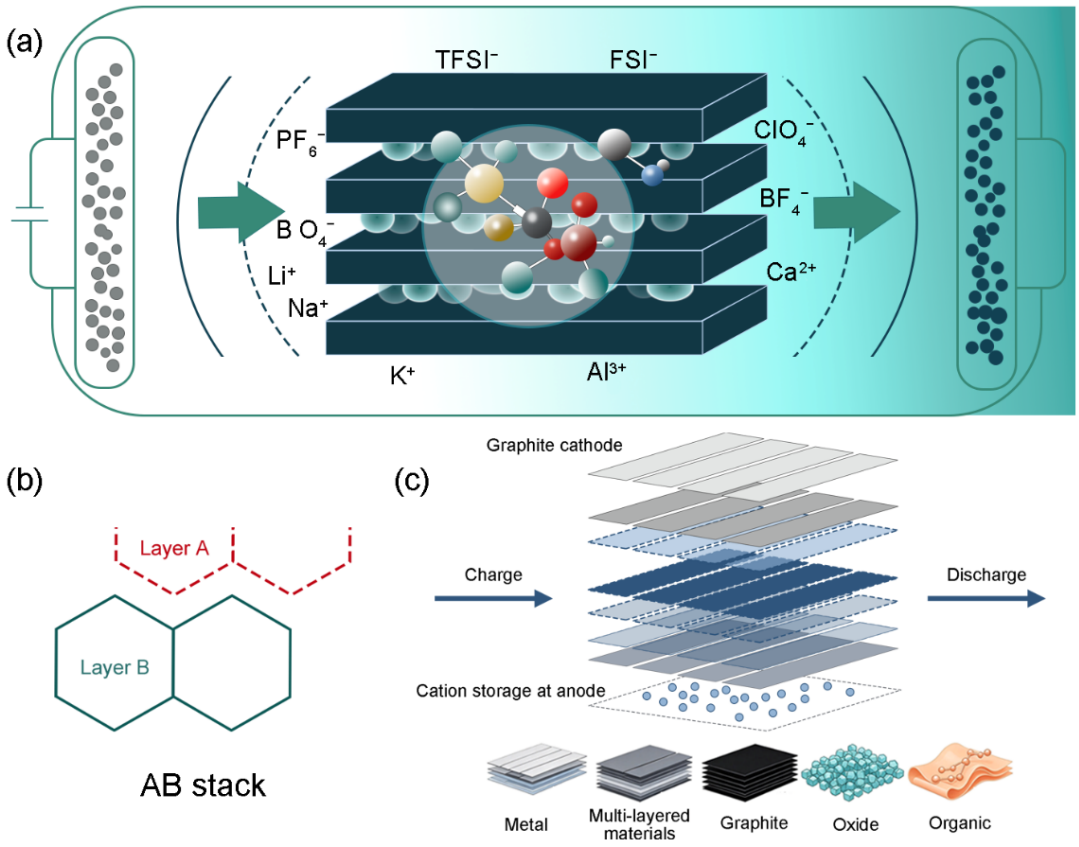


Figure 3. Schematic diagram of the anion storage mechanism for graphite-based dual-ion batteries (**a**), AB-stacked graphite lattice structure (**b**), and corresponding DIB device configurations (**c**).

DIBs exhibit a fundamental distinction from conventional rechargeable ion batteries through their unique capability to facilitate anion intercalation, which significantly enhances the battery's operating voltage [35]. This feature is particularly important because the high-voltage electrodes are imperative to improve the energy density and specific power of the rechargeable battery systems. In these processes, the electrolyte ions are the active species. Usually the electrolyte–separator layer has to be much thicker [36]. The electrolyte formulation is of paramount importance to capacity, cell voltage and storage characteristics. The nature of the anion in the host material is determined by the solvent type, salt concentration, additives and anion type, which all have a strong impact on the reversible capacity, cathode potential and discharge voltage. In addition, the intercalation/deintercalation of anions into/from the cathode material usually occurs at high voltages, which is beneficial for the realisation of enhanced energy density. In general, the anion intercalation and de-intercalation in graphite show a low voltage hysteresis, which results in a high voltage efficiency and energy efficiency.

The cathode materials are the key to determining the basic electrochemical properties of batteries, such as the working voltage window and energy storage capacity. As the host structure for reversible lithium (de)intercalation, these materials govern the battery's performance through their intrinsic electronic/ionic conductivity, structural stability during cycling, and redox reaction thermodynamics. Recently, researchers have explored various anion hosting cathodes and integrated them with different cation hosting or metal-based anodes in dual-ion battery configurations. Currently studied DIB materials include cathodes such as graphitic carbons, MOFs, organic electroactive polymers, and MXenes, along with anodes such as metal anodes (Li, Na, K), intercalation-type materials (graphite, amorphous carbon, TiO_2, MoO_3, MoS_2), alloying metals (Sn, Si), and activated carbon, as summarized in Figure 3b,c [37–41]. Carbon-based materials are considered as very promising candidates for energy storage applications due to their good compromise between cost-effectiveness, natural abundance and electrochemical performance. The DIBs based on graphite cathode have attracted much research attention due to their unique non-transition metal architecture, providing both cost-effectiveness and eco-friendliness. The electrochemical properties of these systems are remarkable, in particular the fact that they present an average operating potential higher than 1.4 V vs. standard hydrogen electrode (SHE). The most suitable cathode material for DIBs is highly orientated pyrolitic graphite, while alternatives such as glassy carbon, carbon fibres and carbon black have been scarcely used. The electrochemical performance of graphite cathodes during anion intercalation is more strongly influenced by GD and crystal quality than for conventional Li^+ intercalation. The structure, morphology, and particle size of graphite strongly affect the anion intercalation behaviour. Better graphitisation and crystal order improve capacity and cycling stability, suggesting that a well-structured graphite framework is favourable for anion intercalation. The two-dimensional zero-gap semimetallic structure of graphite allows charge delocalisation and stabilisation, allowing electron accumulation in the antibonding π^*-band or hole formation in the bonding π-band [42]. Such a unique electronic configuration allows for the concurrent intercalation of anions and cations, thus promoting the development of GDIBs. Xie et al. proposed a novel one-step carbonisation strategy to accurately tune structural disorder in graphite cathodes (Figure 4a) [43]. Using catalytic graphitisation, chemical activation and heteroatom doping with moderate-temperature treatment (<900 °C), they produced carbon materials with well-defined graphitic domains and engineered disorder characteristics such as vacancy defects, nitrogen dopants and micropores. This rational design of disorder architecture offers dual charge storage mechanisms, i.e., conventional anion intercalation in conjunction with enhanced surface-mediated capacitive storage. The optimised SDG-800 cathode exhibits excellent electrochemical performances with a record high capacity of 264 mAh g^{-1} at 0.2 A g^{-1} and superior rate capability (94 mAh g^{-1} at 2.0 A g^{-1}) and cycling stability (>1400 cycles).

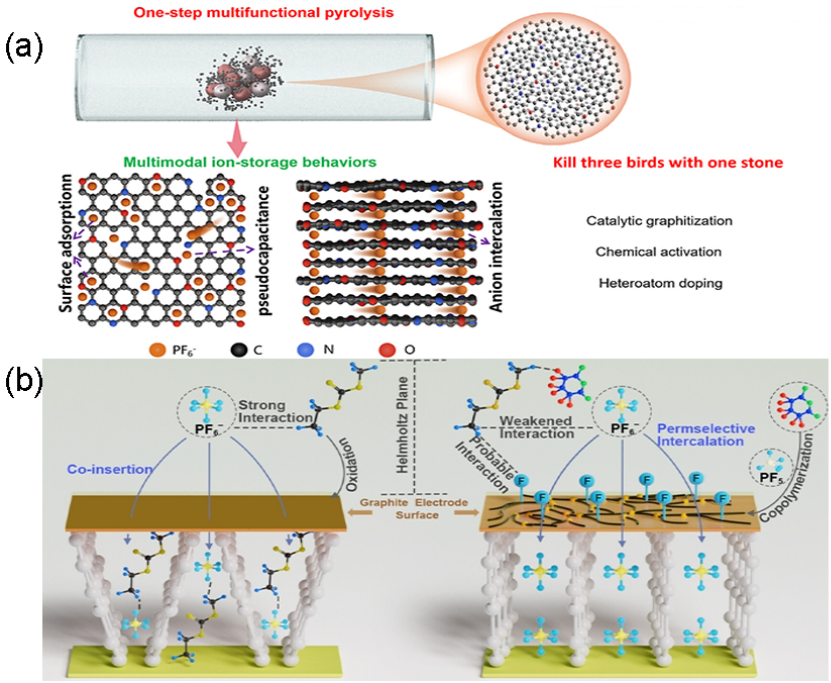


Figure 4. (**a**) Architecture and working principle of SDG-x cathodes (Reproduced with permission from ref. [43]. Copyright 2026, John Wiley and Sons); (**b**) working mechanism of PF_6^- intercalated graphite cathodes during DIB charging (Reproduced with permission from ref. [44]. Copyright 2025, John Wiley and Sons).

The growing concerns of resource scarcity and environmental sustainability of conventional battery metals (especially Li, Co and Ni) have accelerated the search for alternative electrode materials. Organic electrode materials have therefore emerged as next-generation candidates, possessing three unique features: reliance on earth-abundant elements (C, H, N, O), cost-effective synthesis routes, and theoretical energy densities of >700 Wh kg^{-1} [45]. Their structural adaptability is a remarkable feature that enables reversible accommodation of different charge-compensating ions in electrochemical processes, leading to compatibility with multiple battery configurations while retaining optimal performance indicators. Organic electrode materials are classified into n-type and p-type systems based on their redox mechanism. The n-type materials are mainly involved in reduction processes via electron acceptance at their LUMO, which inherently limits their operational potentials to relatively low values (typically <3 V vs. Li^+/Li). This potential limitation thus hampers their practical pairing with conventional graphite anodes, due to thermodynamic incompatibility. Conversely, p-systems are observed in reduced states natively and undergo oxidation processes donating electrons from their highest occupied molecular orbitals (HOMO). This redox property allows p-type materials to attain much higher working potentials (>3 V vs. Li^+/Li) while remaining electrochemically compatible with the standard anode materials. Organic cathodes, compared to inorganic ones, depend on redox processes at the molecular scale, where electron storage is accomplished by frontier orbital transitions (HOMO-LUMO) of discrete molecules and ion storage is accomplished by reversible intercalation of charge-balancing species into functional groups. The molecular makeup of organic materials (crystalline or amorphous) gives rise to intrinsic void spaces that act as universal hosts for a variety of charge carriers (e.g., Li^+/Na^+/K^+ cations or PF_6^- anions) in single-molecule redox reactions. For DIBs, the p-type and n-type organic electrodes suffer from intrinsic trade-offs among specific capacity, operating voltage and cycling stability [46–48]. Furthermore, most reported organic electrodes show promising performance at low mass-loading conditions, while poor charge transport would significantly degrade the capacity and rate performance at practical high mass loadings.

Anode materials are equally important as cathodes in DIBs since they determine the key performance parameters such as rate capability, cycling stability, and capacity by selectively storing and releasing cations via mechanisms similar to rocking-chair batteries [49–51]. Any host materials capable of reversible cation storage can be potentially used as DIB anode [52–54]. Based on the reaction mechanisms with host materials, DIB anodes can be divided into metallic, alloying, intercalation, conversion and adsorption types [55–57]. Basically, an anode can be any host material that is capable of reversibly hosting a given cation. Traditional materials that have long been used for lithium-ion or sodium-ion batteries are among the anode materials. The storage kinetics of anions have been shown to be much superior to those of cations, regardless of whether the process is pseudocapacitive or diffusion limited. The origin of this kinetic advantage is not yet fully understood, but is in part ascribed to the much lower desolvation energy barrier of anions that only weakly interact with solvent molecules in solution, which often limits the storage of cations. The anode material should be compatible with the cathode to achieve the best electrochemical performance. For example, the anode kinetics must match the rapid capacitive anion intercalation process at the cathode [58]. Tang et al. developed an innovative carbon microdomain engineering approach to construct high-performance anodes with ion-mediated nitrogen-active sites and molecular-scale closed-pore structures to overcome the kinetic mismatch between conventional carbon anodes with sluggish ion transport and graphite cathodes with fast capacitive anion intercalation [59]. Experimental and theoretical investigations demonstrate that the designed oxidised nitrogen species can efficiently facilitate Na^+ desolvation and consequently improve the Na^+ storage kinetics of the closed-pore structures. These tailor-made pores also offer abundant Na^+ storage sites, thus improving plateau capacity. This method is a good trade-off between the rate performance and the plateau capacity [60]. The DIB system with engineered anode and expanded graphite cathode exhibits excellent cycling stability with 80.6% capacity retention after 10,000 cycles at 10 C and excellent rate capability. This performance sets a new record among the reported SDIB systems.

3. Intercalation Chemistry in Graphite

Graphite materials are made up of rings of sp2-hybridized carbon atoms, with aromatic planar rings that are stacked in layers stabilised by π-π interactions in the electronic structure [61]. Graphite consists of hexagonal carbon rings stacked on top of each other with weak interlayer forces. This layered structure allows ion intercalation/deintercalation during cycling. This is further supported by the interlayer distance of graphite of about 3.35 Å which allows the intercalation and deintercalation of ions. Graphite is generally used as anode for cation insertion and cathode for anion intercalation. This structural property is exploited for charge storage. During charge, different ions are inserted into the layers of graphite to create specific types of GICs. In GICs new covalent bonds are formed that disrupt the π-electron system of graphite resulting in a distorted layered structure and lower electrical conductivity. Meanwhile, adverse anion solvation at the Helmholtz plane encourages the co-intercalation

of carbonate solvents into graphite upon charging, enabled by strong H–F attraction to PF_6^-. Oxidation of the resulting carbonate–PF6 pairs yields gas and causes structural collapse of graphite cathodes (Figure 4b) [44].

At certain values of the chemical potential, anions or cations can overcome van der Waals forces and intercalate between the graphite layers, forming staged structures. The concept is based on the assumption that a uniform GIC phase exists in a defect-free graphite lattice, originating from the balance between the van der Waals attraction between the graphene layers and the Coulombic repulsion within and between the anion layers, as discussed in the Rüdorff and Daumas Hérold models. The intercalation process of Li^+-intercalated graphite is described by three stages, 0.2 V for formation of stage-IV compounds, 0.12 V for transition from stage-III to stage-II (LiC_{12}), and 0.08 V from stage-II to stage-I (LiC_6). The phase-I (LiC_6) is related to the maximum theoretical capacity (372 mAh g^{-1}) under standard conditions. According to the Rüdorff and Daumas-Herold models, fewer carbon layers between adjacent intercalant layers allow greater ion insertion, resulting in higher electrode capacity (Figure 5a) [62]. X-ray diffraction, dilatometry, chemical analysis, and NMR have been used to elucidate the structure of PF_6^- intercalates, including interlayer spacing, molecular orientation, and anion composition. A sequence of stages, originating from the $C_{24}PF_6$ composition, develops during charging. Ultimately, at full charge, the structure converges to a $C_{20}PF_6$ stage I configuration, characterized by PF_6^- anions closely interacting with graphite layers and approximately 0.7 cointercalated solvent molecules (Figure 5b) [63]. Assuming complete intercalation of 1 mol of LiPF6 into graphite to form $C_{20}PF_6$, this process involves the transfer of 1 mol of electrons, with one PF_6^- ion associated with 20 carbon atoms. Consequently, the theoretical specific capacity limit is approximately 112 mAh g^{-1}.

The development of advanced DIBs stems from early research on anion intercalation into graphite to form acceptor-type GICs. The initial study on acceptor-type GICs involved applying fuming sulfuric acid to graphite in carbon-containing steel. The observed swelling was later identified as H_2SO_4-GIC, marking the first reported case of anion intercalation into graphitic carbon. Anion intercalation involves distinct stages marked by changes in the repeat distance of layer I (spacing between layers with intercalated anions) and gallery height d (distance between graphene layers). These stages correspond to the formation of GICs at various charge/discharge potentials and capacities. Over the past decades, the reversible intercalation and deintercalation of anions (such as PF_6^-, BF_4^-, ClO_4^-, $AlCl_4^-$, $CF_3SO_3^-$, and $C_6H_5COO^-$) into and from graphite have been extensively studied [64]. Currently, most cathodes are graphite-based materials, enabling anion intercalation and deintercalation during charge and discharge due to their layered structure of hexagonal carbon rings with weak interlayer forces (Figure 5c) [65]. The electrochemical performance of graphite cathodes during anion intercalation/deintercalation is more strongly affected by graphitization degree and crystal quality than in traditional Li^+ intercalation processes. Enhanced graphitization and crystal order typically result in increased charge/discharge capacity and improved cycling stability, indicating that a well-structured graphitic framework favors anion intercalation [66]. Smaller anions require lower intercalation potentials to expand graphite layers, potentially leading to higher theoretical capacity. However, this principle does not apply universally to all anions.

Graphite cathodes store ions through intercalation, but their capacity is constrained by limited intercalation sites. Current studies indicate that both the degree of graphitization and the surface characteristics of graphite particles significantly influence reversible anion intercalation and de-intercalation processes. Larger anions have restricted intercalation into graphite layers, further reducing the theoretical capacity. For instance, PF_6^- has a size of 4.36 Å, significantly larger than Li^+ at 0.76 Å, which corresponds to a theoretical capacity of 112 mAh g^{-1} for $C_{20}PF_6$ [67]. Moreover, the intercalation of larger anions induces considerable volume expansion in the graphite cathode (over 130%), potentially leading to exfoliation and capacity degradation [68]. To enhance anion storage, it is essential to increase the intercalation sites within the cathode and incorporate additional storage mechanisms. To enhance the electrochemical performance of common graphite materials, structural engineering and surface modification (such as interlayer spacing enlargement or active functional groups introduction) can be applied. Surface treatments and functional binders improve cycling stability and structural robustness. Heteroatom doping and surface functional groups increase the number of active sites for anion storage. The electrochemical activity of anion intercalation into graphite is limited to the potential range of 4.5–5.0 V, intercalation starting at 4.5 V. Depending on the properties of the graphite, the formulation of the electrolyte and the cycling temperature, the practical PF_6^- storage capacity can be as low as 20 mAh g^{-1} and as high as 150 mAh g^{-1} (Table 1). It was also found that graphite intercalated with PF_6^- anions generally intercalates at potentials up to 4.6 V vs. Li^+/Li. The high voltage process caused decomposition of the standard organic electrolytes. Moreover, the large ionic radius of the anions resulted in structural damage to the graphite layers and exfoliation of graphene sheets, leading to capacity degradation during cycling. For multicomponent electrolyte systems, the situation is more complicated, because the solvation chemistry is controlled by at least two factors, i.e., competitive/cooperative solvent-anion interactions in the bulk electrolyte and preferential interfacial selectivity of graphite cathodes to certain solvated

anion species during charge transfer [69]. Esters are major solvent candidates for DIBs because of their advantageous physicochemical properties. An important study investigating the intercalation of PF_6^- into graphite cathodes in an ethylene carbonate/ethyl methyl carbonate (EC/EMC) binary solvent system revealed co-solvent effects that were clearly distinguishable, with ethylene carbonate acting as an inhibitor and EMC promoting the intercalation process. However, poor oxidation stability limits the practical use of carbonate-based electrolytes, which calls for the development of next-generation electrolyte formulations. In particular, low-viscosity carboxylic esters have attracted significant interest as alternative solvents for rechargeable battery systems. Previous studies have shown that methyl acetate has low viscosity, but poor oxidation stability and can cause excessive PF_6^- intercalation in graphite cathodes. In recent studies, the addition of EMC to methyl acetate-based electrolytes has improved the electrochemical performance, however, the fast capacity fading has not been solved so far [70]. Table 1 summarises the electrochemical performance of graphite-based dual-ion batteries reported in recent studies with graphite used as either the cathode or the anode under different electrolyte systems.

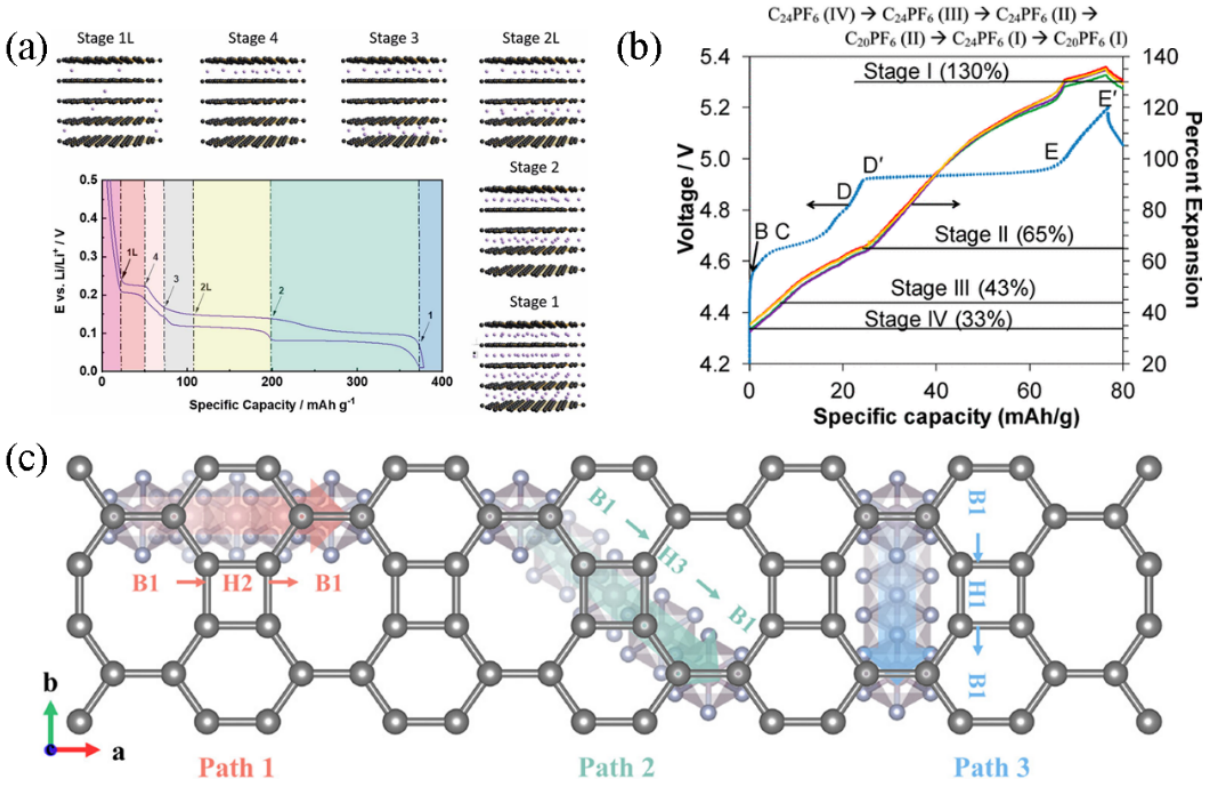


Figure 5. A schematic depiction of the staging mechanism involved in the electrochemical intercalation and deintercalation processes of lithium cations (**a**) and PF_6^- anions (Reproduced from ref. [62] under the Creative Commons Attribution 3.0 Unported License (CC BY 3.0)); (**b**) within graphite (Reproduced with permission from ref [63]. Copyright 2015, American Chemical Society); (**c**) graphical depiction of three configurational diffusion channels with respective kinetic parameters (Reproduced with permission from ref. [65]. Copyright 2025, American Chemical Society).

Table 1. Summary of electrochemical performance and research development of graphite-based dual-ion batteries with various material and electrolyte systems.

Anode Material	Cathode Material	Electrolyte	Working Potential (V)	Specific Capacity (mAh g^{-1})	Rate Capacity	Cyclability (Cycles/Capacity Retention)	Ref.
Graphite	PPYDPZ	5 M $LiBF_4$ in EC/DMC (*v*/*v* 1:1)	2.1–4.4 (vs. Li/Li^+)	151 mAh g^{-1} at 0.1 A g^{-1}	94 mAh g^{-1} at 5 A g^{-1} (≈25 C)	1600 cycles/79% capacity retention/2 A g^{-1}	[45]
Graphite	P(PZ2TPA-TPP)	1 M $LiPF_6$ in EC/DEC/EMC (*v*/*v*/*v* 1:1:1)	2.4–4.3 (vs. Li/Li^+)	140 mAh g^{-1} at 0.2 A g^{-1}	87% capacity retention after 16,000 cycles	600 cycles/87% capacity retention	[48]
Zn metal	N-doped carbon	30 M $ZnCl_2$ water-in-salt electrolyte	1.6–1.95 (vs. Zn/Zn^+)	134 mAh g^{-1} at 0.1 A g^{-1}	~75 mAh g^{-1} at 0.1 A g^{-1}	800 cycles/1 A g^{-1}	[71]
Graphite	PETCZ poly(9″-ethyl-9H,9″H-3,3′:9′,3″-tercarbazole)	5 M $LiClO_4$ in EC/DMC (*v*/*v* 1:1)	1.9–4.1 (vs. Li/Li^+)	159 mAh g^{-1} at 0.2 A g^{-1}	147 mAh g^{-1} at 0.5 A g^{-1}	4500 cycles/76% capacity retention/3 A g^{-1}	[64]
Mn-PAA/Graphite	$LiCoO_2$	1 M $LiPF_6$ in EC/DMC (*v*/*v* 1:1)	1.2–4.0 (vs. Li/Li^+)	1.88 mAh g^{-1} at 0.1 C	1.08 mAh g^{-1} at 2 C	50 cycles/80% capacity retention/0.2 C	[72]
RP/NMG	N-doped mesoporous graphene	1 M $NaPF_6$ in EC/EMC/DEC/DMC (*v*/*v*/*v*/*v* = 1:1:1:1)	2.5–4.2 (vs. Na/Na^+)	89 mAh g^{-1} at 0.1 A g^{-1}	66 mAh g^{-1} at 0.5 A g^{-1}	1000 cycles/92% capacity retention/0.5 A g^{-1}	[73]
Mg metal	Graphite	9 M $MgCl_2$ + 30 M ChCl aqueous deep eutectic solvent	1.1 (vs. Ag/AgCl)	151 mAh g^{-1} at 0.1 A g^{-1}	——	280 cycles with average CE of 99%	[74]
Hard carbon	O-FeCl intercalated graphite	Sodium-based electrolyte containing PF_6^-	2.0–5.0 (vs. Na/Na^+)	110 mAh g^{-1} at 0.2 A g^{-1}	Capacity decay < 0.02% per cycle over 1000 cycles at 1 A g^{-1}	>1000 cycles	[75]
Zn metal	Graphite	4 M $Zn(OTf)_2$ in DPM/water mixed solvent + 5 wt.% VC additive	0.2–2.4 (Zn/graphite full cell)	140 mAh g^{-1} at 0.1 A g^{-1}	84.2% after 500 cycles at 100 mA g^{-1}	500 cycles at 0.1 A g^{-1}	[76]
Te at porous carbon nanofibers	Graphite	KFSI/TEP-FTEP (TEP:FTEP = 5:1 volume ratio, LHCE)	3.5–5.25 (vs. K^+/K)	45 mAh g^{-1} at 0.5 A g^{-1}	39.9 mAh g^{-1} at 0.5 A g^{-1}	100 cycles (0.1 A g^{-1})	[77]
PTCDI	Graphite	3.9375 M LiTFSI aqueous electrolyte with FEC additive	0–2.55 (vs. Li/Li^+)	47 mAh g^{-1} at 0.285 A g^{-1}	26 mAh g^{-1} at 50 mA g^{-1}	1000 cycles/90% capacity retention	[78]
Co-BDC	Graphite	[EMIm]Br + LiTFSI in DME/DOL (*v*/*v* 1:1)	0–3 (vs. Li/Li^+)	226 mAh g^{-1} at 100 mA g^{-1}	101 mAh g^{-1} at 500 mA g^{-1}	500 cycles/67% capacity retention/0.2 A g^{-1}	[79]
Li metal	Graphite	2 M $LiPF_6$ in EMC electrolyte with Tris(trimethylsiloxy)boron (TMSB) additive	3.0–5.2 (vs. Li/Li^+)	82.18 mAh g^{-1} (1 C)	84.21% capacity retention	2000 cycles/87.86% capacity retention/50 C	[80]
Graphite	Graphite	LiFSI-3TMS-3TTE (LHCE, molar ratio); Contrast: HCE (LiFSI-3TMS), LCE (LiFSI-8TMS)	3.0–5.2 (vs. Li/Li^+)	109.2 mAh g^{-1} at 0.5 A g^{-1}	100~500 mA g^{-1}; Excellent rate property	1000 cycles/99%/0.2 A g^{-1};	[81]
MCMB graphite	Graphite	3 M $LiPF_6$ in EMC + 3 vol% TMSP additives	3.0–5.0 (vs. Li/Li^+)	101.3 mAh g^{-1}	101.3 mAh g^{-1} at 0.1 A g^{-1}	3000 cycles/92.5% capacity retention/1 A g^{-1}	[82]

4. Charge Carriers for GDIBs

The application of DIBs extends beyond the high energy density of graphite-graphite electrode architectures. A key advantage is their material sustainability relative to conventional high-voltage battery systems. The all-graphite DIB architectures do away with the need for scarce, expensive or environmentally harmful materials from the entire battery system. This advantage is especially important for sodium, potassium or multivalent metal salts (e.g., Al, Ca, Mg or Zn) instead of lithium in both electrolyte formulations and electrode designs, allowing for the possibility of more cost-effective and sustainable DIB systems [83].

4.1. Anionic Charge Carriers

The majority of anion intercalating species in carbon based materials have larger ionic radii than alkali and alkaline metal ions, limiting the number of active sites in the cathode for anion storage. Therefore, the smaller number of intercalated anions between graphene layers decreases the theoretical specific capacity. The principal processes of anion intercalation and de-intercalation in the graphite matrix occur at potentials above 4.5 V vs. Li/Li^+. Zhou and Sit using first-principles calculations showed that the trend for molecular intercalants to enter graphite follows the order of: $BETI^- > FSI^- > FTFSI^- > FSI^-/TFSI^- > TFSI^- > TFSI^-/FSI^-$ [84]. The unfavourable anion solvation dynamics under hydrothermal processing conditions hinder the electrochemical co-intercalation of solvent species, like carbonates, into graphite during charging. This is largely attributed to the high affinity of these anions for PF species via hydrogen–fluoride interactions. A key factor is the ion desolvation energy, the energy needed to remove specific anions from the electrolyte. The desolvation energy is inversely related to the size of the ion, meaning that smaller anions need more energy to be desolvated. One important parameter is the intercalation energy, which is the energy required to incorporate anions into the graphite lattice. Compared to the desolvation energy, this parameter increases linearly with the size of the anion, because a larger anion requires more energy. The larger the anion size, the higher the charging voltage needed to accommodate the expansion of the interlayer space during intercalation. First-principles calculations demonstrate that the propensity of molecular intercalants for graphite intercalation follows the order: $PF_6^- \gg BF_4^- > TFSI^- > AlCl_4^- > ClO_4^-$. Earlier studies have indicated that an increase in the cathode cut-off voltage improves the intercalation capacity of anions. Higher cut-off voltage could promote oxidative degradation processes in the DIB cell, which would lead to reduced Coulombic efficiency (CE). Very high voltage limits can oxidise the electrolyte and form an insulating layer on the graphite surface, which hinders the effective transport of anions. The ionic conductivity at 20 °C showed an increasing trend with decreasing ion size in the order: $BETI^- < TFSI^- < TFSI^-/FSI^- < FTFSI^- < FSI^-/TFSI^- < FSI^-$. These observations indicate that the electrochemical diffusion properties of the anions are mainly governed by ion pairing and self-aggregation phenomena in the electrolytes. In addition, the concerted anion–solvent co-intercalation mechanism has been demonstrated, where PF_6^- anions and their coordinated EMC molecules co-intercalate into graphite as an integrated unit [85]. The comparative analysis of the calculated intercalation energies (Figure 6a) clearly demonstrates the thermodynamic gain of PF_6^--EMC co-intercalation over isolated PF_6^- anions.

The halogen-ion storage mechanisms provide a promising route for the development of next-generation battery technologies (Figure 6b) [79]. This approach utilises the reversible transport and storage of halide anions between electrodes, enabling the development of halide-ion battery systems with remarkable theoretical volumetric energy densities. The small ionic sizes and adjustable redox potentials of halogen ions (Cl^-, Br^-, I^-) facilitate effective redox reactions in various electrolyte environments. Throughout cycling, small halogen ions effectively intercalate and deintercalate from the graphite electrode's interlayer spaces within a voltage window of 0–3 V (vs. graphite). The integration of halogen electrochemistry with lithium intercalation/deintercalation exhibited notable reversibility in the assembled graphite symmetric DIBs. Few studies have explored DIB systems using single halide ions as charge carriers, likely because traditional designs utilize graphite for both the cathode and anode. Experimental results indicate that direct reversible chlorine insertion into graphite does not occur. Instead, bromine or iodine can serve as effective chemical mediators to facilitate chlorine intercalation into graphite layers. The halogen anions in the electrolyte function both as charge carriers and electroactive species for electrode reactions. NFG cathodes, possessing a high specific surface area (~1000 $m^2\ g^{-1}$), demonstrate superior kinetic performance for dual-halogen storage [86]. This few-layer graphitic cathode facilitates both conversion and intercalation reaction pathways. However, the underlying dual-halogen storage mechanism requires further investigation to achieve a comprehensive understanding.

Incorporating multivalent halide anions (e.g., Zn-Cl and Mg-Cl) into cathode materials leads to higher capacity compared to monovalent anions. These species enable the formation of novel GICs. A systematic study of their intercalation mechanisms could greatly improve the performance of electrodes and help in designing advanced host materials. The intercalation of $AlCl_4^-$ anions leads to fast electron transfer on the external circuit

and the formation of neutral $AlCl_4^-$ molecules. The intercalated $AlCl_4$ molecules in GICs have been proposed to adopt different possible geometries, either square planar or tetrahedral configurations, which is still under debate in previous studies. The diffusion energy barrier of $AlCl_4^-$ in graphite is relatively low, which is about 0.012~0.029 eV. Computational results show an intercalant gallery height of 8.36–8.76 Å, large enough to accommodate the van der Waals radius of $AlCl_4$ (~5.95 Å) and maintain C-Cl distances of 3.15–3.25 Å [87]. For GICs, the tetrahedral configuration of $AlCl_4$ is more stable (0.69 eV lower in energy) than planar geometries. In particular, both $AlCl_4$ anions and neutral $AlCl_4$ molecules are found to be of higher energy in a planar configuration than in a tetrahedral one, even in preintercalation vacuum conditions. To go from tetrahedral to planar geometry energy barriers of 1.74 eV for $AlCl_4^-$ and 0.77 eV for $AlCl_4$ have to be overcome. Furthermore, the lying conformation of tetrahedral $AlCl_4^-$ is energetically preferred by 0.08 eV in comparison to the standing one.

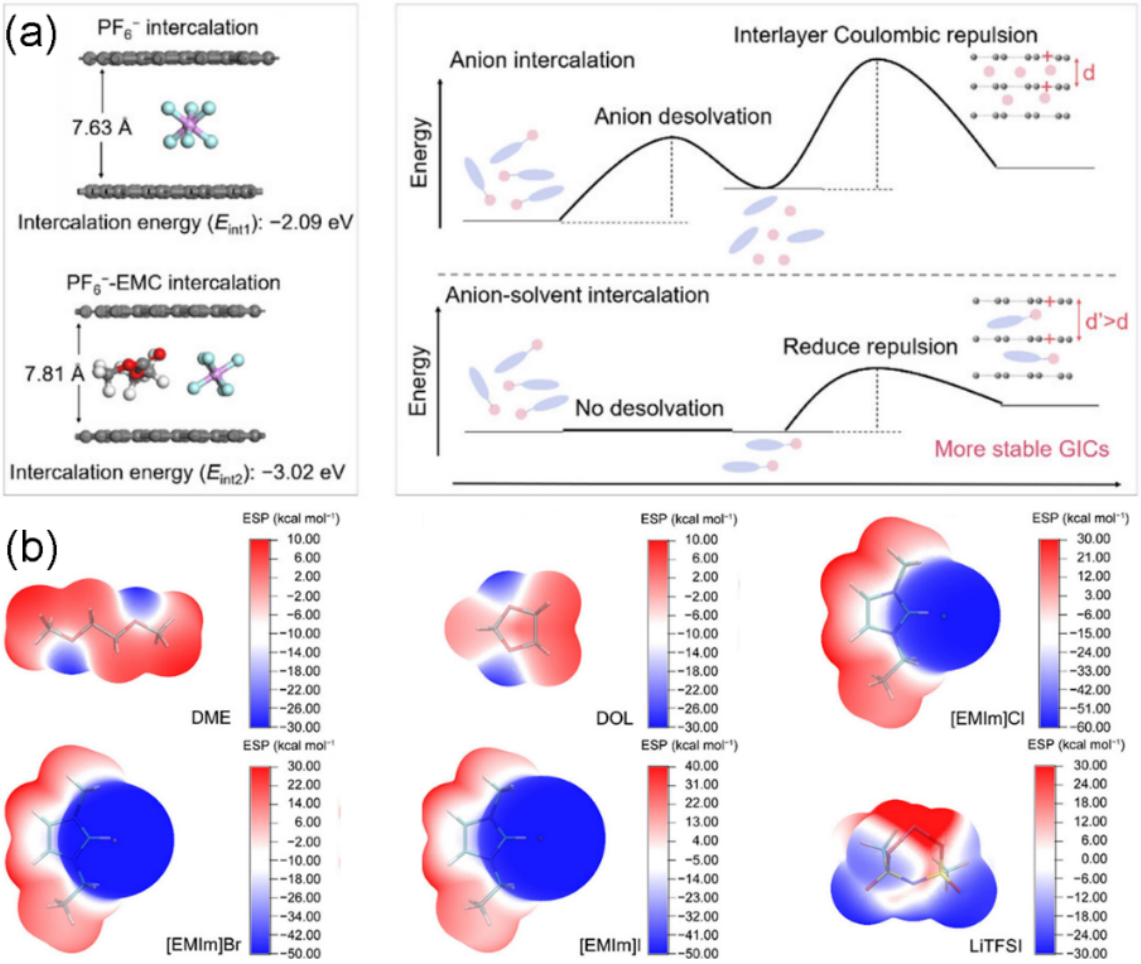


Figure 6. (**a**) Intercalation of anions in graphite cathodes (Top: DFT-calculated geometries and intercalation energies of $C_{20}[PF_6^-]$ and $C_{20}[PF_6^-$-EMC] GICs; Bottom: Thermodynamics of solvated vs. bare PF_6^- intercalation.) (Reproduced with permission from ref. [85]. Copyright 2025, John Wiley and Sons); (**b**) Halogen-based dual-ion battery mechanism MESP mapping of electrolyte components in Li/halogen systems (Reproduced with permission from ref. [79]. Copyright 2025, American Chemical Society).

4.2. Cationic Charge Carriers

Recently, there has been a surge in research interest in the development of alternative battery technologies that use abundant and low-cost cations such as K^+, Na^+, Ca^{2+}, Mg^{2+}, Al^{3+}, Zn^{2+} and nonmetallic ions such as NH_4^+ and H^+ [88]. This increasing research emphasis is in line with the global trend of sustainable, low-carbon energy solutions and looks for ways to overcome limitations of conventional LIBs using more accessible resources [89]. Repeated lithium intercalation/deintercalation in LIBs results in structural degradation of the graphite anode, such as layer expansion and surface oxidation. This structural expansion weakens the interlayer van der Waals forces in cycled graphite and makes it much more susceptible to further oxidation than pristine commercial material. Interestingly, this pre-oxidized state of spent graphite enables the synthesis of graphene oxide with reduced oxidant requirement, indicating an efficient recycling pathway [90]. Although there has been significant progress, the long

charging time of today's electric vehicles is a major obstacle to mass adoption because it does not match the convenience of refuelling conventional vehicles. This fundamental limitation is due to the anisotropic nature of graphite anode materials in LIBs, which greatly limits Li^+ ion transport across graphene layers during intercalation/deintercalation [91]. In particular, the sluggish Li^+ interfacial diffusion kinetics at graphite interlayers is the main limiting factor for high-rate performance. A key research direction to address this challenge is the development of high-power battery systems that can be charged at ≥10 C rates (full charge in <6 min). The unique advantages of SDIBs make them a promising energy storage technology. These include high operating voltages, plentiful sodium resources and environmental friendliness due to non-transition metal cathodes [92]. These advantageous properties together make SDIBs particularly promising for large-scale energy storage applications. Graphite is a poor anode material for SDIBs because it does not intercalate Na properly and electrolytes that are suitable decompose at high voltages [93]. The reaction mechanism of DIBs is similar to that of conventional "rocking-chair" batteries, but the electrolyte systems for DIBs are remarkably different.

The high natural abundance of potassium (2.09 wt.% vs. 0.0017 wt.% of lithium) and favourable redox potential of the K/K^+ couple (−2.93 V vs. E_0), close to that of Li/Li^+ (−3.04 V vs. E_0), make KDIBs promising for large-scale energy storage [94]. Compared to cation intercalation in metal-ion batteries, anion intercalation in KDIBs generally occurs at higher voltages (>4.2 V vs. K/K^+), enabling high energy density. Some graphite-based electrodes have dual-ion storage ability, in which anions and cations are stored simultaneously, leading the construction of KDIBs and improvement of the working voltage plateau (>3.8 V vs. K/K^+) in full cells. Most of the carbon materials (e.g., hard carbon) have large intrinsic limitations such as low specific capacity, which severely affect the stability of potassium-ion full cells [95]. Research efforts on KDIBs have been mainly focused on the development of carbonaceous anode materials, due to their great potential for practical implementations. However, present KDIBs using carbonaceous anodes and graphite cathodes have low capacity (<100 mAh g^{-1}, anode-based) and poor cycling stability. This is mainly due to the large volume change during the K^+ intercalation/deintercalation, which is related to the large ionic radius of K^+ ion. Graphite anodes expand by ~60% on K^+ intercalation and PF_6^- intercalation results in ~140% expansion of the cathode. These large dimensional changes lead to destabilisation of the solid electrolyte interphase layer and deterioration of the electrochemical performance. Such challenges have motivated the development of effective strategies such as nitrogen doping to improve the performance of carbonaceous anodes. The introduced nitrogen defects not only enhance the electronic conductivity but also facilitate the reversible K^+ storage, leading to the excellent capacity and cyclability. In addition, hierarchically structured carbon materials can accommodate volume changes, which thus enhance long-term cycling stability. Electrospun hierarchical porous N-doped carbon fibres have been proposed as an integrated anode material for KDIBs, with three unique structural merits, including flexible and binder-free properties for mechanical robustness, interconnected multichannel porosity for fast K^+ diffusion and electron transfer, and enough void space for volume variation and solid electrolyte interphases (SEI) layer stability [96]. These structural merits lead to outstanding electrochemical performance with a high working voltage of 4.4 V, excellent cycling stability (197 mAh g^{-1} at 50 mA g^{-1} after 90 cycles), and superior rate capability (57.0 mAh g^{-1} at 250 mA g^{-1}). These comprehensive performance indicators demonstrate the technological promise of N-doped carbon fibres as a candidate anode for next-generation KDIB systems. The freeze-dried 3D porous dipotassium terephthalate (pK_2TP) nanosheets possess enhanced electrochemical kinetics and cycling durability, offering a breakthrough in organic electrode engineering [97]. The nanostructured pK_2TP shows enhanced K^+ storage properties with faster ion diffusion ($D_{K^+} = 10^{-9}$ cm^2 s^{-1}) and improved charge transfer over the bulk counterparts due to its interconnected conductive network. They have achieved unprecedented performance in KDIBs using this anode with expanded graphite cathode (pK_2TP//EG): 20 C rate capability and 100% capacity retention over 2000 cycles, which is state-of-the-art for KDIB systems. *Ex situ* spectroscopic studies (FTIR/Raman) corroborate the reversible redox process between carboxylate (K_2TP) and enolate (K_4TP) states upon PF_6^-/K^+ co-intercalation. The optimised pK_2TP//EG configuration shows 68 mAh g^{-1} at 2 C and surpasses conventional K_2TP and previous KDIB benchmarks in both rate performance and cycle life, implying a feasible strategy for sustainable energy storage.

One of the factors limiting the large-scale application of LIBs for energy storage is the scarcity of lithium resources. Na-ion and K-ion batteries have attracted extensive attention due to their natural abundance, but their energy density is still unsatisfactory. Unlike these monovalent systems, systems with multivalent ions show multi-electron redox features that could be beneficial for energy capacity [98]. As mentioned before, the reaction kinetics of the reacting cations are very important to determine the electrochemical performance of DIBs, in particular the rate capability [99]. Non lithium cations such as Ca^{2+} (ionic radius: 1.00 Å) have large ionic radii and thus suppress such kinetic behaviours strongly. Different strategies have been exploited to improve the electrochemical performances of alloying anodes in lithium-based DIBs (e.g., aluminium), but similar modifications of alloying anodes for non-lithium cations (e.g., tin) are seldom reported. Thus, improving the reversible reaction kinetics of

alloys with non–lithium cations for anodes is of great importance for the development of low–cost and high–performance DIBs. Potential strategies include: engineering and tuning anode architectures to enable faster ion transport; designing new high-capacity anode materials for non-lithium cations; and employing new reaction mechanisms with improved kinetics, for example, adsorption/desorption processes, to improve the overall electrochemical performance. Aluminium is the most abundant and cost-effective element of those used in DIBs on Earth after graphite, in terms of natural abundance and cost [100]. The element aluminium (electron configuration: $1s^2 2s^2 2p^6 3s^2 3p^1$) belongs to the space group Fm3m. The three valence electrons in this structure are highly mobile and this gives rise to an electrical conductivity of 3.8×10^7 S m^{-1}, which is ~65% of that of copper. Aluminium is more stable to air and water than lithium or sodium [101]. The interaction between anions and cations and the cointercalation of electrolyte solvents may lead to exfoliation and destruction of the graphite structure, limiting the specific capacity and long-term cycling performance of the DIBs. The incorporation of Al^{3+} ion into the cathode represents the transfer of three electrons, that is, a three-electron reduction process. High charge transfer is difficult to be handled for conventional cathodes because of the cation radius variation caused by valence changes and lattice structure disruption, which leads to poor cycle stability. Al^{3+} is very Lewis acidic which restricts its incorporation into graphite and other materials. In particular, usage of anions such as $AlCl_4^-$ as an active species rather than free Al^{3+} can alleviate volumetric and structural stresses during cycling. Ca-based batteries are attractive because calcium is naturally abundant and has a relatively low redox potential of Ca/Ca^{2+} (−2.87 V vs. SHE), which is lower than that of other metals (e.g., Mg/Mg^{2+} at −2.37 V, Al/Al^{3+} at −1.66 V, and Zn/Zn^{2+} at −0.76 V), making possible high-voltage battery systems [102]. Layered structure graphite has been widely used as the cathode materials in Zn dual-ion batteries [103–105].

5. Electrolytes

The electrolytes of DIBs are similar to LIBs and can be crystalline solids, ionic liquids, polymers, or liquid media. It is better to use liquid or polymer electrolytes as they make a good contact with electrodes. For liquid electrolytes, the electrochemical stability window is determined by the energy gap between the highest occupied molecular orbital (HOMO) and lowest unoccupied molecular orbital (LUMO) [106]. A higher LUMO level means more resistance to reduction, and a lower HOMO level means better stability against oxidation. For a stable cell, the anode and cathode potentials should be well matched to the LUMO and HOMO levels of the electrolyte, respectively. In DIBs, intercalation of anions occurs at relatively high potentials. Graphite cathodes coupled to low potential anodes usually demand an electrolyte which is electrochemically stable over 5 V. Therefore, it is crucial to investigate the electrolytes that can maintain the stability under such high voltage conditions for reliable performance [107]. The electrochemical stability window (ESW) is generally mainly determined by electrolyte solvents. For example, graphite anodes generally require EC solvent, but graphite cathodes are strongly inhibited in anion intercalation by EC solvent. However, EMC and DMC prefer larger intercalation capacities of anions, but have a limited ability to form stable SEI. In addition to providing ionic charge carriers and enabling reversible cation reactions at the anode, an ideal electrolyte should also enable high-capacity, reversible anion intercalation at the cathode. High electrolyte concentration reduces the volume and mass of the battery and improves the full-cell DIB energy density, whereas a high ionic conductivity is important for better rate performance.

Anions also suffer from a solvation effect analogous to cations that may limit battery performance. Larger size of anions causes weaker anion–solvent and anion–cation interactions, resulting in a lower “solvation effect” and lower desolvation energy barrier than cations. The “solvation effect” process links anion intercalation to solvent molecules, which can decompose at the cathode if they have low oxidation stability. Also, if the anion–solvent interaction is strong enough, the anions can drag solvent molecules into the graphite cathode, which splits the layers and exfoliates the graphite structure. This leads to decrease of CE, intercalation capacity and cycling stability. Electrolytes made solely from salts and solvents often struggle to simultaneously provide the high oxidative and reductive stability essential for DIB operation [108–110]. To balance electrolyte compatibility at both electrodes, in addition to optimizing solvents and salts, incorporating functional additives offers an effective solution. Selective decomposition of additives at either the anode or cathode promotes the formation of SEI or cathode electrolyte interphases (CEI) layers, which help prevent electrolyte solvent breakdown and stabilize electrode/electrolyte interfaces [111]. Overall, suitable electrolytes for DIBs should meet the necessary requirements. First, a high electrochemical stability of the electrolyte, especially of the graphite-intercalated anions, is essential for ensuring reversible anion intercalation/de-intercalation and extending cycle life. Moreover, like LIBs and other rocking-chair cells, the electrolyte must be compatible with the anode for effective SEI formation and with inactive cell components like the Al current collector.

The operating voltages of aqueous GDIBs are determined by the competition between the anion intercalation energy and the hydration energy, representing the balance between the anion-graphite host interactions and the anion-water solvation [112]. Systematic analysis showed that the electrochemical performance is dominated by the trade-off between the anion intercalation energy and the hydration energy. Aqueous DIBs have been developed greatly recently. A metal–free system consisting of a 3,4,9,10-perylenetetracarboxylic diimide (PTCDI) organic anode and a graphite cathode has been developed [113]. Extensive studies of anion intercalation behaviour were conducted on three different anion species ($TFSI^-$, Otf^- and BF_4^-) using their sodium–based electrolytes. The PTCDI-graphite system in NaTFSI electrolyte showed excellent electrochemical properties with a discharge plateau of 2.2 V and a capacity of 120 mAh g^{-1}. The mechanism of energy storage was revealed by advanced characterisation techniques, such as *in situ* X-ray diffraction and Raman spectroscopy, which gave direct evidence for intercalation of $TFSI^-$ into the graphite host.

Traditional organic solvent-based electrolytes face problems like safety, environmental impact and cost. In response, there has been a growing interest in aqueous and hybrid aqueous-organic electrolyte systems that offer promising alternatives to solve the drawbacks of conventional non-aqueous electrolytes, as reported in recent research [114]. Several strategies have been proposed to improve the ESW of aqueous electrolytes by suppressing water decomposition with promising results. These approaches have been developed into sophisticated formulations like hydrate-melt electrolytes, water-in-bisalt systems, water-in-ionomer configurations, and hybrid aqueous/non-aqueous electrolytes, all of which have shown significantly widened ESWs [115]. Quasi-solid-state batteries have appeared as a promising candidate for next generation EES systems [116]. The quasi-solid-state electrolytes (QSSEs) display rapid ion conduction at room temperature (10^{-4}–10^{-3} S cm^{-1}) leading to fast charge/discharge kinetics in the assembled devices [117]. Furthermore, because of their large ESW (>5 V) and excellent chemical compatibility, they are especially well suited for high-energy battery architectures that use high-voltage cathodes and lithium metal anodes. In addition, the intrinsic non-flammability and leak-proof nature of QSSEs significantly contribute to battery safety. Hence, quasi-solid-state dual-ion batteries (QSS-DIBs) are under active development as a cost-effective and robust energy storage technology. In conventional QSS-DIBs, earth-abundant graphite cathodes are used for reversible anion storage/release at high operating potentials (>4.5 V vs. Li/Li^+). However, their practical application is hindered by the limited ion transport kinetics in QSS-DIBs, leading to limited areal capacities (<0.2 mAh cm^{-2}) on graphite cathodes. High-areal-capacity graphite electrodes are important for commercial viability to offset the parasitic mass and volume contributions from inactive components (e.g., binders, current collectors, and packaging materials). Development of high-loading graphite cathodes to overcome this limitation is a critical step toward realisation of practical QSS-DIB applications. However, DIBs still suffer from the low CE and the gradual loss of capacity, mainly due to the interfacial side reactions and the structural degradation of graphite during the cycling of high-voltage anion intercalation. Surface modification has been suggested as a promising approach to stabilise the CEI and decrease the graphite structural damage. Graphite cathodes have been coated with different materials, e.g., alumina, lithium titanate, and artificial anode-electrolyte interphases. However, such insulating coatings inevitably hinder both electronic and ionic transport, which is a key barrier to be overcome for high areal capacity in QSS-DIBs.

6. Limitations and Optimization Strategies

6.1. Limitations

6.1.1. Material-Level Limitations

Insufficient capacity remains a significant barrier for commercialisation of dual-ion battery systems. The large ionic radii of anions (3.9 Å for $TFSI^-$, 4.36 Å for PF_6^- and 5.28 Å for $AlCl_4^-$) together with limited interstitial sites result in a low theoretical specific capacity (112 mAh g^{-1} for $C_{20}PF_6$) and poor energy density in DIBs using conventional layered cathodes such as graphite. Thus, enhancing the specific capacity of cathodes and the overall energy density of DIBs is still a major research goal. The possible directions are (a) design advanced carbonaceous materials with higher specific capacities, (b) explore other layered materials, such as two-dimensional layered compounds, which may overcome the issues of low specific capacity in DIBs, and (c) integrate cathode materials with intrinsically high specific capacities, such as main-chain benzidine polymers (165 mAh g^{-1}), tetrathiafulvalene derivatives (196 mAh g^{-1}) and porphyrinoids (200 mAh g^{-1}).

The relatively slow reaction kinetics of non-lithium cations poses a major challenge. As mentioned above, the electrochemical performance of DIBs, particularly the rate capability, highly depends on the reaction kinetics of the involved cations. The large ionic radii of the non-lithium cations, 1.02 Å for Na^+, 1.38 Å for K^+, and 1.00 Å for Ca^{2+}, severely hamper these kinetics. Various strategies have been applied to improve the electrochemical performance of alloying anodes in lithium-based DIBs, while similar modifications of alloying anodes for non-

lithium cations are seldom reported. Therefore, improving the reversible reaction kinetics of anodes that alloy with non-Li cations is crucial for the progress of low-cost, high-performance DIBs. Possible approaches include: designing and engineering anode structures for faster ion transport; developing new anode materials with higher capacity for non-lithium cations; and using new reaction mechanisms with improved kinetics, e.g., adsorption/desorption, to improve overall electrochemical performance.

CE is an important metric to evaluate the reversibility of charge-transfer during battery cycling. However, the problem of high CE for DIBs is still very challenging, especially in the first few or several dozens of cycles. High CE means lower electrolyte consumption due to reversible active material loss, which reduces system cost and weight, and improves commercial viability. The anion intercalation reaction is a partially irreversible process because of the relatively large size of the anion that induces a trapping phenomenon. Secondly, the operating voltage up to 5 V causes continuous side reactions, such as electrolyte decomposition and degradation of electrode materials. These processes are major contributors to the low CE, often below 90%, observed in DIBs. These phenomena are especially prominent at the exposed edges of the graphite cathode, where electrolyte decomposition not only depletes active materials but also leads to the formation of a thick, uneven interfacial layer. This layer elevates interfacial resistance and further diminishes CE. Gas evolution caused by electrolyte decomposition accelerates graphite cathode damage, leading to irreversible capacity loss. Co-intercalation of solvents and the irreversible removal of anions or solvent molecules further impair CE.

High operating voltages cause ongoing electrolyte decomposition and reduce CE. As anions serve as charge carriers in the intercalation process, their depletion indicates a decline in electrochemical performance, stemming from restricted intercalation and deintercalation activities. Frequent de/intercalation of numerous anions and solvents can severely damage the cathode structure, leading to diminished cycling stability. Furthermore, when anions are stabilized within their solvation shells, the electrolyte's oxidative stability diminishes, which can accelerate the breakdown of the graphite electrode during solvent intercalation. Developing stable interfaces and electrolytes is an effective strategy for mitigating these challenges. Forming a stable CEI membrane offers a practical approach to enhance CE [76]. A robust and compatible CEI can suppress side reactions, minimise electrolyte depletion and avoid solvent intercalation. Moreover, the overall efficiency can be improved by tuning the solvation environment of the anion to facilitate the desolvation at the interface. *In situ* preparation of CEI film on cathode graphite surface is the key approach to enhance the electrochemical performance of DIBs [118]. The selection of appropriate electrolyte additives or pretreatment methods is key to suppress side reactions, protect the graphite structure from decomposition products, and form a stable, thin and uniform CEI layer (Figure 7) [80]. These measures will be pivotal for improving the durability, power density and cycle life of DIBs under high-voltage and extreme temperature conditions [119,120]. Besides *in situ* CEI formation via electrolyte decomposition, there is great potential for advancement with artificial interface engineering on the cathode surface. Modification of the cathode surface improves structural stability by minimising cracking and CEI rebuilding due to volume changes during anion insertion/extraction, thus improving overall battery performance [121].

Metal foils and carbon-based materials are predominantly used in DIBs, where current collectors are key components of battery architectures. Commonly used current collectors for cathode preparation are aluminium foils (density ≈ 2.7 g cm^{-3}) and carbon cloths (theoretical density ≈ 2.2 g cm^{-3}). Usually, the anode architectures come from aluminium foils or copper foils or carbon cloth substitutes, which make the electrode assembly a variety of options. However, conventional metal current collectors in DIBs have a number of inherent limitations for implementation. First, the high density of metallic collectors (more than 2.2 g cm^{-3} for graphite) greatly reduces the active material mass fraction to less than 40% in composite electrodes, thus largely degrading the specific capacity and energy density. Second, the metal components have low electrochemical stability and are heavily corroded during long cycling. Third, the anion intercalation process results in a large (>80%) volume expansion of the cathode, which cannot be effectively accommodated by rigid metal foils, leading to mechanical stress and cycling stability issues. These basic limitations, combined, impede the electrochemical performance and practical feasibility of metal-based DIB configurations. To overcome these key challenges, Zhou et al. fabricated an ultra-lightweight three-dimensional carbon current collector (3D CCC) for all-carbon electrodes in both cathode and anode applications, which is a significant improvement in conventional metal foil (Al/Cu) current collectors [122]. The 3D CCC architecture demonstrates multiple merits such as improved electrochemical performance with specific capacities of ~140 mAh g^{-1} at 0.5 C and ~120 mAh g^{-1} at 1 C, respectively, improved energy density normalised to the total electrode mass owing to its lightweight conductive framework, excellent long-term cycling stability over 1000 cycles at 5 C, no electrochemical corrosion at both electrodes, and significant mitigation of cathode volume expansion by its porous buffering structure as directly visualised by *in situ* microscopy. Such synergistic improvements make the 3D CCC a revolutionary design strategy for the realisation of cost-effective, high energy density DIBs with concurrent electrochemical and mechanical stability to overcome the intrinsic limitations of graphite-based electrode systems.

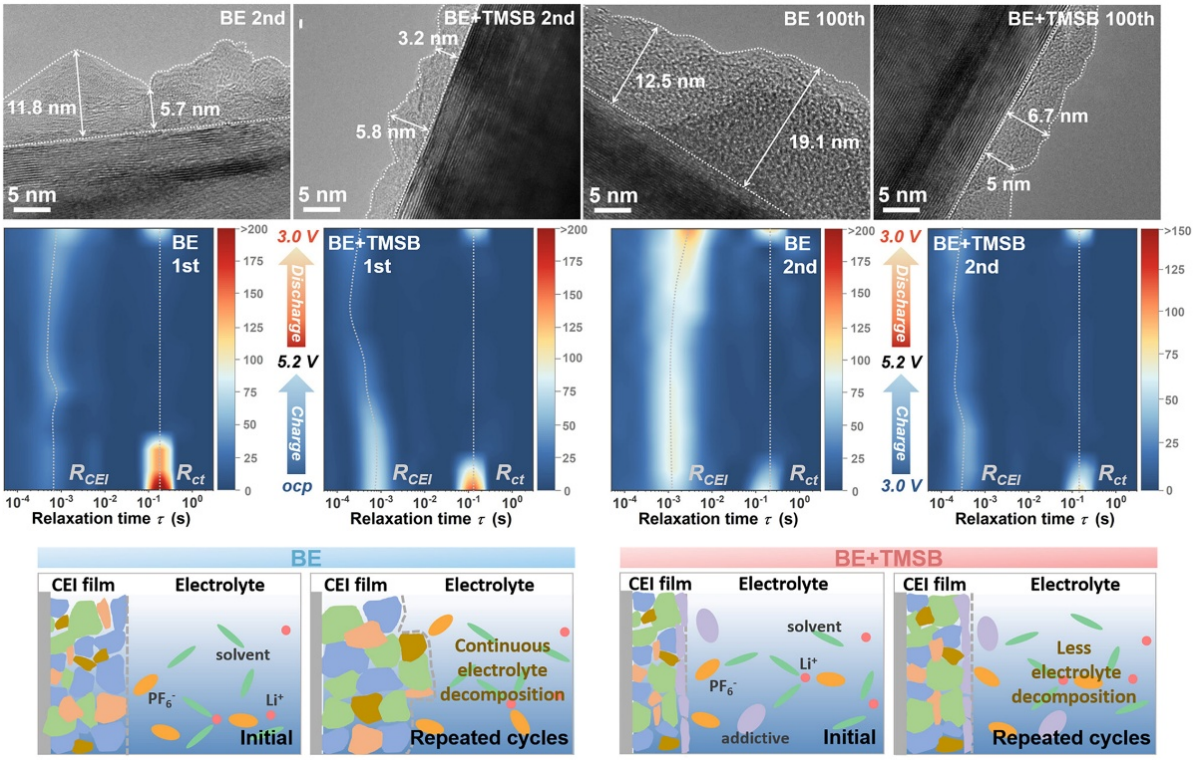


Figure 7. CEI ion transport and structural evolution: HRTEM of graphite in BE vs. BE$^+$TMSB electrolytes (**Top**), EIS-DRT analysis of initial cycling (**Middle**), and mechanism of CEI evolution impacting ion transport (**Bottom**) (Reproduced with permission from ref. [80]. Copyright 2025, American Chemical Society).

6.1.2. Bottlenecks toward Practical Full-Cell Commercialization

In full cells, the negative–to–positive (N/P) ratio is critical for realizing the optimal material performance [123]. An N/P ratio below unity (<1) causes metallic Li/Na/K plating on the anode owing to insufficient anode capacity, triggering dendrite growth and concomitant safety hazards. By contrast, an N/P ratio greater than 1 corresponds to excess anode material, which reduces the initial ICE and cell energy density. Therefore, balancing the N/P ratio is essential for dual–carbon full cells to reconcile safety and energy density. Moreover, since the electrolyte serves as a limiting active component, the electrolyte volume–to–active material mass ratio (E/S) acts as a critical evaluation parameter governing practical cell performance. Adequate salt supply is essential to sustain reversible anion intercalation. Nevertheless, a high E/S ratio introduces substantial dead mass and volume into full cells, deteriorating practical gravimetric and volumetric energy densities at the device level. Reducing the E/S ratio while preserving sufficient active anion species remains a formidable trade–off for DIB full–cell development.

Balancing the kinetic properties of cathode and anode constitutes another critical challenge. Limited anode kinetics substantially restrict the simultaneous realization of high energy density and high power density. Graphite cathodes rely on the intercalation of large-size anions, whereas anodes undergo transport and storage of cations (Li^+, Na^+, K^+ or Zn^{2+}) with distinct ionic radii and diffusion barriers. Rate disparities between anion and cation redox reactions induce uneven local overpotential across electrodes, aggravating parasitic side reactions and accelerating active-ion consumption, which makes it difficult to achieve high energy density and high-power performance simultaneously. For alloying–type anodes such as Al, this issue is further compounded by drastic volume fluctuation and non–uniform alloying reactions during cycling, triggering electrode pulverization. Such inhomogeneous alloying and pulverization of Al anodes become more pronounced when paired with high–areal–loading graphite cathodes (>5 mg cm^{-2}). Therefore, developing uniform Al–based anodes that preserve structural integrity and stability is imperative for matching high–areal–loading cathodes.

Beyond cathode–anode matching, the loss of active cations and anions upon prolonged charge–discharge cycling poses another critical challenge for full–cell design. Analogous to LIBs, DIBs experience anode–side Li loss arising from unstable SEI formation during electrolyte breakdown, dead Li buildup, and irreversible capture by anode defects. This active Li depletion lowers ICE and practical energy density while continuously consuming the Li reservoir, shortening cycle life and raising safety risks. Elevating salt concentration represents a promising strategy, as it supplies extra active cations and anions while strengthening the electrolyte's oxidation resistance and facilitating the generation of both CEI and SEI. Prelithiation, an effective method to boost energy density and

prolong the cycle life of LIBs, is also applicable to DIBs [124]. Meanwhile, high operating voltages exacerbate cathode electrolyte oxidation and massive active anion loss. Additionally, irreversible solvent co–intercalation and adsorption on graphite defects further diminish electrolyte anion concentration. Exploring cathode preanionization additives and overanionized cathode materials constitutes viable strategies to supply supplementary anion sources.

Current laboratory investigations of DIBs rely almost exclusively on performance metrics obtained from coin cells, which frequently cannot be reproduced under practical device configurations. Specifically, nearly all published specific capacities and energy densities are normalized only to active material mass. Such treatment inflates performance metrics relative to practical cells, where electrolyte, current collectors, binders, conductive additives, separators and packaging account for most of the total mass and volume. Practical DIB full–cell development faces multiple constraints originating from device configuration. Gas evolution poses greater intrinsic challenges for DIBs than LIBs owing to their high operating voltages [125]. At such potentials, even minor electrolyte decomposition yields substantial gas volumes. In coin cells, small electrodes and rigid housings mitigate electrode structural degradation to some degree. For pouch cells, however, mechanical constraints over larger electrodes become less homogeneous, inducing severe structural deterioration of electrodes. Beyond the mechanical and gas–related issues arising from cell architecture, high–voltage graphitic cathodes (>4.8 V) encounter material limitations regarding binders. Research dedicated to cathode binder systems for such cathodes remains scarce. Most cathode binders fail to satisfy high–voltage stability requirements owing to premature decomposition. Among existing reports, PVDF is the dominant binder adopted for graphitic cathodes, while CMC is occasionally applied, mostly within full–cell systems. Mishra et al. evaluated the mechanical and electrochemical properties of multiple aqueous binders (namely CMC, SBR, and LgSA) for KS6 graphite cathodes [126]. Their work revealed that the CMC–LgSA blend delivers enhanced adhesion to the current collector and maintains stable cycling during repeated PF_6^- anion intercalation and de–intercalation. Benefiting from the dense electrode coating formed by CMC–LgSA, this binder system exhibits the lowest interfacial resistance originating from current collector contact, interphase evolution and ionic diffusion relative to the other aqueous binders.

6.2. Optimization Strategies for Graphite

6.2.1. Electrode Materials Design

The inherently limited interlayer spacing of graphite (typically ~0.335 nm) restricts anion intercalation kinetics and available active sites. In contrast, graphene–based materials show better performance due to their larger interlayer spacing (typically >0.7 nm) and porous structure which enable better ion diffusion and more active sites. Interestingly, the thermal reduction process can simultaneously induce interlayer expansion and porosity development in graphite derived materials, synergistically enhancing their anion storage capability. More interestingly, reduced graphene oxide undergoes progressive structural amorphization during electrochemical cycling, evolving into a long range disordered configuration. This structural change improves the kinetics of ionic transport by offering more routes for diffusion, and at the same time increases the density of electrochemically active sites [127]. Indeed, the battery presents a typical activation behaviour during the first cycles, gradually increasing its capacity.

Different optimisation strategies have been developed by the researchers to overcome the limited mass transfer efficiency of Li^+ in the graphite anodes. A representative approach is the formation of nanoscale pores by etching and expansion techniques to increase interlayer spacing for improving ionic accessibility [128]. Surface modification with heteroatom doping (e.g., S, N) has also proven to be an effective strategy to enhance Li^+ adsorption capacity and transport kinetics (Figure 8) [129]. However, the intrinsic fast charging limitations of graphite are mainly caused by the slow diffusion of Li^+ through the interlayer channels and suboptimal interfacial reaction kinetics. However, dual-ion battery cathode materials still face great challenges including limited specific capacity and poor rate performance. Such problems are mainly caused by the small number of active sites of cathode and the incongruity of large intercalant anions with the dense graphite framework. To enhance the performance of DIB cathodes, there are mainly two approaches that are studied, which are surface modification of carbon-based cathodes and the discovery of new and advanced cathode materials.

The degree of graphitisation and crystallinity of the carbonaceous materials determine their structural stability, electronic conductivity and energy barriers for ion diffusion. This directly influences the (de)intercalation kinetics of anions in the electrode material. Intercalation chemistry is a versatile approach to tailoring materials by controlled insertion of guest species between the structural layers of host materials, thereby enabling property engineering [130]. The structural order of the sp2-hybridized carbon in cathodes, i.e., the degree of graphitisation (GD), has a significant impact on the anion intercalation. The XRD analysis reveals interlayer spacings of 0.3440 nm (non-graphitic carbon) and 0.3354 nm (ideal graphite) from the (002) peak. Improved GD directly enhances discharge capacity and voltage efficiency, whereas crystallite height (c-axis stacking) has little impact. The effect

of a-axis crystallite size is still unknown. The physical properties of the material, such as particle size and surface morphology, have a strong influence on the electrochemical anion intercalation into graphite cathodes. Larger particles may enhance the structural integrity of the graphite, and thereby improve cycling stability. However, this growth in size also results in a decrease in specific surface area and an increase in the diffusion pathways for anions, leading to a decrease in rate performance and lower specific capacity. Ghosh et al. studied a hybrid strategy combining graphitic intercalation and non-graphitic carbon surface storage to enhance capacity [131]. The electrochemical activity of non-graphitic carbons is determined by specific surface area, pore structure, surface functionalities and doping elements. Systematic optimisation for the determination of the optimum ratio of the graphitic/non-graphitic and the most effective combination of non-graphitic carbon properties for the maximisation of the surface-based storage.

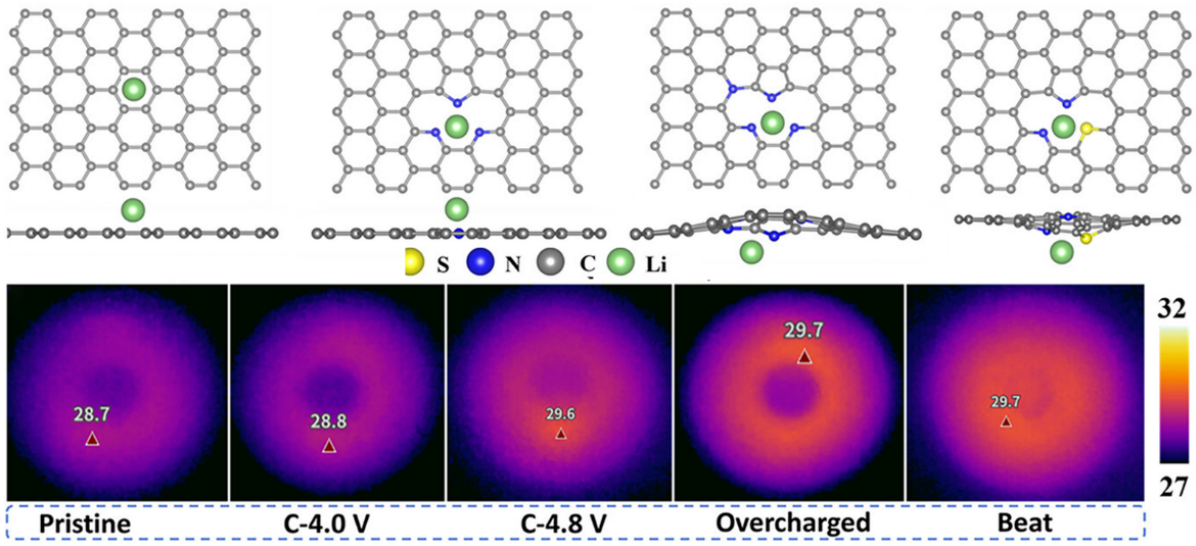


Figure 8. Synthetic route of nitrogen-phosphorus co-doped porous carbon (Reproduced with permission from ref. [129]. Copyright 2026, John Wiley and Sons).

Graphitic carbon cathodes with different morphologies show different anion-storage capacities, and the electrochemical performance is affected by the particle size and the orientation of the graphene layers (Figure 8) [132]. It is to be noted that larger particle sizes will result in longer ion diffusion pathways in the bulk material and thus contribute to slower kinetics of anion intercalation/deintercalation. It is well–known that nanostructured materials have large specific surface areas and facilitate the faster ion transport due to shorter diffusion paths. Therefore, nano–scale modification on graphite can effectively increase the number of active sites and promote the kinetics of intercalation of anions, which is beneficial to the significant improvement of the electrochemical performance of graphite–based electrodes. Nanostructured graphite materials are expected to be more attractive for electrochemical applications because of the faster ion intercalation kinetics that can lead to improved rate performance and cycling stability. Apart from controlling the morphology of graphitic carbon cathodes (e.g., particle size, orientation of graphene layers), the optimised porosity is also important to mitigate the volume expansion caused by ion intercalation via the pore buffering effects. However, excessive pore formation reduces volumetric and gravimetric capacities due to reduced electrode density and increased electrolyte uptake. In contrast, for graphite-based electrodes with inadequate porosity, the volume change during electrochemical cycling is large, leading to poor cycling stability. The porous structure can effectively suppress the volume expansion of the graphitic cathode and provide additional pathways for anion intercalation other than the conventional diffusion pathway.

The specific capacity of carbon-based cathodes depends on the availability of active sites for anion intercalation, while the diffusion dynamics within the interlayer space are closely linked to both active and inactive sites. Increasing the number of active sites can improve the specific capacity of carbonaceous cathodes, while minimising or eliminating the inactive sites can reduce their obstruction effect for anion diffusion. Furthermore, the electronic conductivity of active cathode materials is highly sensitive to the presence of defects and dopants, which in turn directly impacts the reaction kinetics of anions in the cathode matrix. Regardless of the experimental methods developed to reduce the concentration of defects, the defects intrinsic to the graphene layers are unavoidable in the synthesis of graphitic carbon due to the governing thermodynamic principles. These defects are specifically related to the crystalline lattice disorder of graphitic carbon without the incorporation of heteroatoms. The electronic structure of pristine graphitic carbon undergoes modification upon defect formation, thereby

influencing its electrochemical performance. Unlike defect structure modulation in graphitic carbon cathodes, surface functionalization and heteroatom doping strategies incorporate foreign atoms (e.g., O, N, P) into the pristine carbon matrix. Enhancing cathode capacity can be achieved through developing alternative anion host materials, improving graphite cathodes via doping, surface modifications, or expanded graphite, and introducing novel electrolyte anions [133]. An effective coating for ion storage matrices should exhibit anion permeability, optimal porosity and surface area, controllable thickness, chemical stability, suitable wettability, surface homogeneity, mechanical robustness, strong carbon surface adhesion, single-step formability, and facile deposition (like Al_2O_3 as a surface modifier) [134]. Moreover, pitch-derived soft carbon is commonly employed as a buffering matrix for conversion/alloying anodes to accommodate volume variations during cycling. However, surface functionalization still faces the challenge of irreversible graphitic carbon exfoliation during repeated anion intercalation/deintercalation, which significantly limits cycling stability. Introducing heteroatom doping effectively reduces the energy barrier associated with anion embedding and migration processes. Nitrogen doping is generally recognized to enhance electronic conductivity while simultaneously providing additional active sites.

The kinetic disparity between anions and cations, arising from their distinct ionic radii, significantly impacts the performance of dual graphite batteries [135]. More importantly, the slow desorption of large PF_6^- anions at high current rates leads to the irreversible structure damage of graphite cathode, thus resulting in capacity degradation. Moreover, the performance issues are also attributed to the intrinsic drawbacks of graphite cathode materials, such as limited active sites and lack of interlayer spacing for large anions. The interlayer spacing of graphite can be controlled to achieve structural optimisation [136]. Chen et al. developed sulfur-doped graphitized carbon (SGC) through a facile one-step carbonization approach, which simultaneously achieved three key structural features: localized graphitization, porous architecture, and sulfur doping [137]. From the extensive theoretical calculations and material characterisations, they showed that the incorporation of sulphur in the form of C-S-C bonds not only expanded the interlayer spacing but also remarkably enhanced the electrical conductivity of the carbon matrix. Importantly, these C-S-C bonds showed reversible electrochemical behaviour, forming Li_2S at low discharge potentials and converting back during charging, thus allowing for efficient lithium ion storage in DIB cathode. This novel design successfully activated multiple charge storage mechanisms in SGC cathode including anion intercalation, anion adsorption and cation pseudo-capacitance adsorption. GICs show larger interlayer spacings than pristine graphite due to the intercalated species and have shown potential for use in alkali metal (Li, Na, K) ion battery systems. An interlayer-pillar strategy is proposed as an efficient mean to improve the structural stability and cycling performance of graphite, to mitigate the structural degradation induced by repeated anion (de)intercalation. Zhang et al. designed an anion-pillar strategy for graphite cathodes, where the interlayer spacing is effectively expanded and stabilised, alleviating the structural degradation, and efficient anion (de)intercalation is achieved [138]. The SDIB performance of this novel design was excellent, with a capacity of 162 mAh g^{-1} at 200 mA g^{-1} (560 Wh kg^{-1}). The anion pillars retained structural integrity in the graphite interlayers and 74.0% retention with a capacity of 101 mAh g^{-1} (at 2000 mA g^{-1}) was achieved after 15,500 cycles (0.0017% decay per cycle). Xie et al. proposed an electrochemical-mechanical synergistic activation strategy that weakens the interlayer van der Waals forces in graphite [139]. This approach sequentially combines electrochemical interlayer expansion with mechanical shearing, generating lateral stress that substantially reduces interlayer interactions while preserving the covalent carbon framework. The resulting force-modulated graphite offers a dual enhancement in anion storage kinetics and structural integrity, delivering 65 mAh g^{-1} at 20C and significantly outperforming pristine spent graphite, commercial graphite, and high-temperature annealed graphite, while sustaining stable cycling over 2000 cycles at 10C with 91% capacity retention.

6.2.2. Strategies for Stabilizing Electrolyte Interphase Layer

Like the SEI layer on the anode, the CEI layer on the cathode is essential for electrolyte stability and facilitates efficient anion intercalation. In DIBs, the anionic solvation sheaths from the electrolyte adsorb on the graphite cathode surface and partially intercalate the graphitic interlayers during charge-discharge cycling. This starts chemical reactions between specific electrolyte constituents and graphite, resulting in the formation of a CEI layer that coats the surfaces of the graphite particles and continuously interacts with the electrolyte constituents. Modifying electrolyte composition is a very attractive strategy to improve oxidative stability, control interphase formation and change reaction pathways for anion intercalation. Cheng et al. added tris(trimethyl-silyl) phosphite (TMSP) as an electrolyte additive to enhance the electrochemical performance [82]. TMSP can remove the harmful byproducts of electrolyte decomposition and can also form a thin, homogeneous cathode-electrolyte interphase on graphite. Consequently, remarkable improvements of the electrochemical properties are achieved. However, understanding of its composition, formation process, and the evolution during anion intercalation and deintercalation remains limited [140]. Due to their typically larger size compared to cations, anions require the

CEI layer to be sufficiently elastic to accommodate the cathode's volume changes. Additionally, high anionic conductivity is essential to facilitate efficient insertion and de-insertion of anions at the interface. A representative advancement in graphite cathode stabilization involves the development of an anion-conductive polymer interface via metatungstate-doped polyaniline (PANi) coating, fabricated through a cost-effective wet-chemical oxidative polymerization method that exploits π-π stacking interactions for uniform coverage (Figure 9a). The resulting core-shell architecture combines multiple functional advantages: solvated PANi matrix enabling high anion conductivity and structural stability, *in situ* formation of a hybrid CEI that effectively suppresses solvent co-intercalation, and metatungstate doping that enhances electrochemical stability at high voltages (>4.5 V vs. Li/Li^+) while improving charge transport. This design yields exceptional electrochemical performance, including 94% capacity retention after 2000 cycles and a record-high areal capacity of 1.78 mAh cm^{-2} at 0.1 mA cm^{-2} [141]. The surface functionalisation of graphite cathodes by introducing functional groups may improve the stability of CEI layer further. For instance, heteroatom dopants modified graphite accelerates the transport of target ions within the CEI film. Hu and co-workers synthesised several N-doped graphite samples with interlayer distances ranging from 0.39 to 0.51 nm, using a simple one-step scalable catalytic method at 700, 800 and 900 °C [142]. The 800 °C treated sample shows dramatically increased interlayer spacing, providing more space for anion accommodation and significantly enhancing DIB specific capacity. Electrochemical characterisation together with theoretical calculations confirmed the synergistic effects of heteroatom doping, such as enhanced anion adsorption, reduced migration barriers and optimised anion diffusion paths. Moreover, the selection of well-designed binders can improve the interfacial affinity between electrolytes and graphite cathodes, and thus enhance the structural stability of the CEI film. Binders that are capable of covering enough of the surface of the active-material particles can suppress the decomposition of the solvent and reduce solvent co-intercalation, which causes damaging exfoliation in the graphite lattices [143]. Research efforts devoted to exploring high-performance binders for graphite-based cathodes in DIB systems are relatively scarce. In general, a desirable CEI layer is expected to modulate anion-conducting properties, facilitate anion transport across the electrolyte-electrode interface, and reduce the overall internal resistance of the battery.

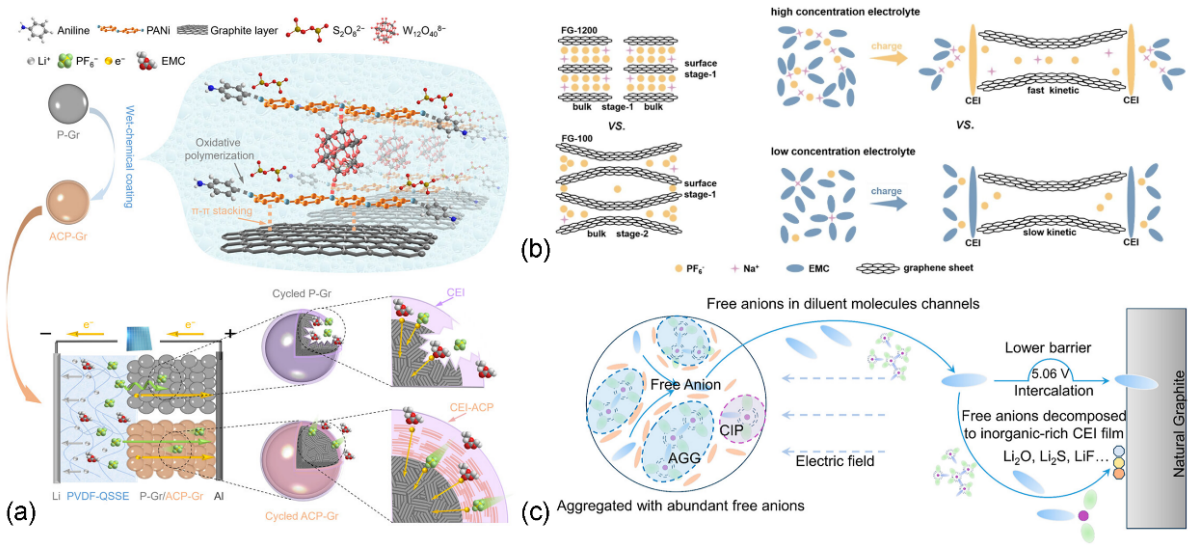


Figure 9. (**a**) Formation of metatungstate-doped PANi/CEI hybrid layer on graphite: constructed via oxidative polymerisation and π-π stacking, confined electrolyte oxidation, conductive CEI-ACP interface, dual-function: suppresses side reactions and enhances anion transport (Reproduced with permission from ref. [141]. Copyright 2024, American Chemical Society). (**b**) Dual interfacial effects during charging: Surface effect: CEI formation dynamics and concentration effect of ion redistribution at electrode interface (Reproduced with permission from ref. [144]. Copyright 2025, John Wiley and Sons). (**c**) Carbon layer restructuring in SDIBs: structural evolution during electrochemical cycling and correlation with Na^+ intercalation kinetics (Reproduced with permission from ref. [81]. Copyright 2025, American Chemical Society).

6.2.3. Electrolyte Design

The development of high-performance DIBs needs the electrolytes with several essential characteristics to achieve both electrochemical superiority and practical feasibility. The most crucial of these requirements is outstanding oxidative stability (3.0–5.2 V vs. Li^+/Li), which is necessary to enable reversible anion intercalation

during high-voltage operation [145]. Equally important is the fact that the electrolyte is concentrated enough (>2 M, salt-dependent) to afford sufficient ionic conductivity and to promote efficient charge storage in graphite-based electrodes [146]. In terms of materials interface, electrolyte should have dual functionality: one is to passivate aluminium current collectors effectively and the other is to promote the formation of robust SEI and CEI interphases for enhanced cycle life. Furthermore, the considerations of industrial applicability make the combination of economical feasibility (cheap, abundant materials) with environmental sustainability (green solvents and salts) for electrolyte components, particularly in the case of large-scale deployment [147]. These multifunctional properties of electrolytes collectively constitute important criteria for the progress of practical dual-ion battery technologies. Several approaches based on electrolyte have been proposed to improve the stability of graphite cathode. They include the use of ionic liquid electrolytes, the implementation of highly concentrated electrolyte solutions, the incorporation of gel polymer electrolytes, and the supplementation of specific electrolyte additives [148]. Future DIB research should be directed toward the development of sustainable electrolyte systems, in particular aqueous-based chlorides and metal-chloride complexes. The intrinsic reduction of oxygen content due to the exclusion of transition metal oxides from cathodes is a critical factor, since oxygen availability is directly responsible for thermal runaway propagation. The design philosophy naturally improves safety by reducing the number of components that support combustion. Moreover, concentrated electrolytes are inherently safer than conventional dilute systems, primarily due to the reduced amount of flammable solvent. The concentration effect is referred to the preferential coordination of anions with cations over solvent molecules, which facilitates the formation of anion-derived stable CEI and facilitates anion intercalation as shown in Figure 9b [144]. Also, high-concentration electrolytes (HCEs) exhibit: decreased volatility, enhanced thermal stability, and suppressed flammability. Notably, HCE formulations enable the incorporation of non-flammable cosolvents (e.g., phosphates or water) that are incompatible with dilute electrolytes, thereby further mitigating fire risks [149].

Electrolyte composition and concentration strongly influence the availability, intercalation dynamics, and interfacial evolution of cations and anions during extended cycling. HCEs have been formulated to ensure an adequate ion supply and extend the ESW, thereby enhancing the performance of GDIBs. However, the elevated viscosity and cost associated with HCEs hinder their practical application by impairing ion transport kinetics. Additionally, HCEs tend to promote the formation of highly aggregated coordinated ion pairs, which facilitate solvent co-intercalation and result in the progressive depletion of anions within the electrolyte. To attain low desolvation energy, a stable interface, and an effective intercalation energy barrier—considered the rate-determining steps for high-performance DIBs—the solvation environments of cations and anions should be tailored through the use of locally concentrated electrolytes (Figure 9c) [81].

Existing studies on DIB additives primarily aim to form stable CEI layers by suppressing solvent decomposition through preferential decomposition pathways in HCEs. Nevertheless, escalating the salt concentration to improve performance results in higher overall battery costs, posing challenges to the practical deployment of DIBs. In electrolytes with comparable solvation structures but varying salt concentrations, the graphite cathode demonstrated similar PF_6^- anion intercalation characteristics. Developing low-concentration electrolytes offers the opportunity to tailor the solvation environment, enhancing the stability of anion deintercalation at high voltages and ensuring compatibility with the cathode material. Incorporating functional additives such as ethylene sulfite and vinylene carbonate into electrolytes can facilitate anion intercalation into graphite, thereby enhancing capacity and cycling stability. For example, the addition of fluoroethylene carbonate alters the solvation structures of Na^+ cations and PF_6^- anions, leading to significantly enhanced electrochemical stability of the electrolyte and the development of robust, stable electrode-electrolyte interphase layers. Functional additives play a crucial role in stabilizing electrode/electrolyte interfaces by preferentially undergoing redox reactions at cathode and anode surfaces [150]. These additives facilitate the formation of robust CEI/SEI layers with tailored chemical compositions and multifunctional properties, effectively suppressing electrolyte decomposition and minimizing parasitic side reactions during battery cycling. However, most conventional electrolyte additives are primarily designed to optimize cathode performance while neglecting their adverse effects on anode interfacial chemistry. For example, nitrile (-CN) and phosphate ester (PE) additives have been shown to enhance cycling stability and interphase properties on high-voltage cathodes, but they often inadvertently increase overall cell impedance due to unfavorable interactions with anode materials. Additives designed to passivate the graphite anode in DIBs must undergo decomposition at potentials lower than those of the solvent, thereby generating a dense, anion-permeable interfacial layer. The formation of a CEI must precede anion intercalation into graphite to effectively suppress solvent co-intercalation and prevent structural exfoliation of the graphite electrode [151].

In contrast, additives containing fluorine and silicon such as (pentafluorophenyl)triethoxysilane, (3,3,3-trifluoropropyl)methylcyclotrisiloxane and dimethoxymethyl(3,3,3-trifluoropropyl)silane show better

bifunctional properties. These compounds not only stabilise high voltage cathodes, but also optimise SEI formation on anodes leading to significant improvements in overall electrochemical performance. The fluorine fragments in these additives can be dissociated and react with Li^+ to form LiF, which can improve the interfacial mechanical stability. Moreover, polymerisation of fluorine-derived decomposition products produces fluorinated polymers with wide band gaps and low electron affinity, further improving CEI/SEI stability while maintaining high ionic conductivity at the electrode interfaces. The newly developed electrolyte additive ethyl 2,2-difluoro-2-trimethylsilylacetate exploits the cooperative interaction between silicon and fluorine functional groups to simultaneously enhance the performance of both $LiCoO_2$ cathodes and graphite anodes [152]. Conventional additives have their advantages but are typically only for a particular function and for one electrode (cathode or anode), which limits their scope for improving the overall battery performance [153]. To solve these problems and meet the increasing demands on high performance, recent works have been devoted to the design of novel multifunctional electrolyte additives that can simultaneously enhance the cycle stability, rate capability and safety features [154].

7. Challenges and Perspectives

The review provides an in-depth analysis of the dual-ion battery technology, focusing on three main aspects: material optimisation, system level development, and performance evaluation. As we can see, the engineering of graphite electrodes has been remarkably developed, especially in terms of tailored microstructure modifications and optimised electrolyte formulations for anion storage and cycling stability (Figure 10). Still, there remain stubborn problems, particularly regarding interfacial degradation and long-term electrochemical reversibility. In this review, some future perspectives and potential research directions for advancing the dual–ion battery technologies are highlighted, offering helpful insights for practical applications.

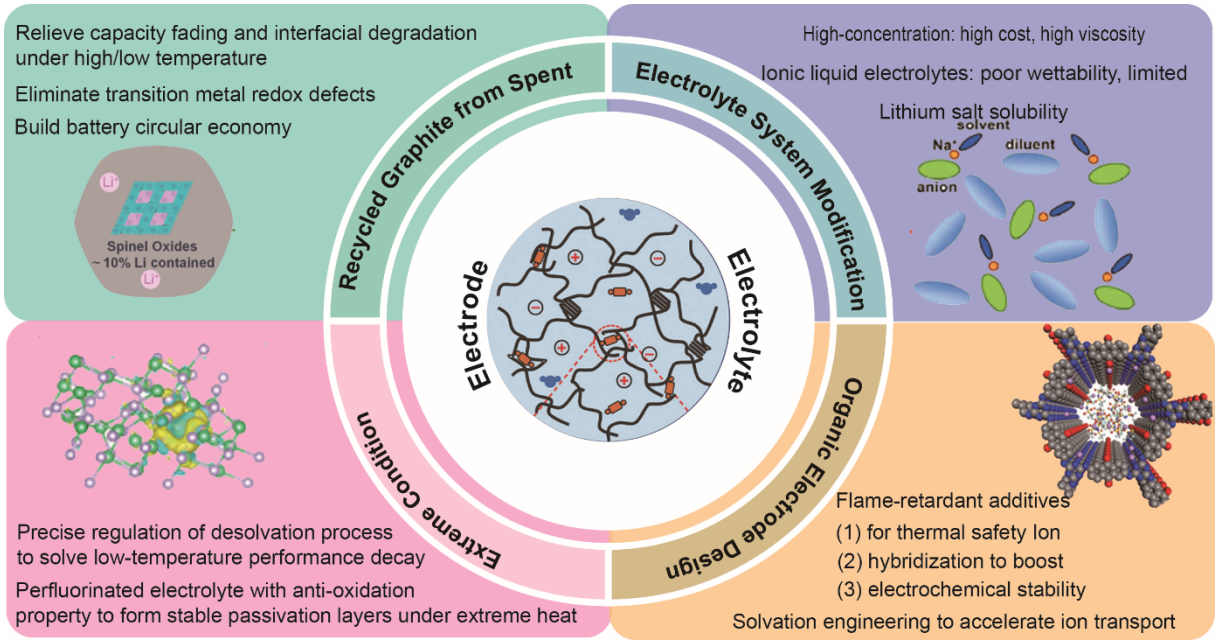


Figure 10. Challenges and perspectives of dual-ion battery.

(1) High-concentration and ionic liquid-based electrolytes offer a wide ESW for high-voltage anion intercalation, but practical issues such as high cost, viscosity, poor wettability, and low solubility of lithium salts (<1.5 M) limit their practical application. Recent progress in the modification of organic electrolytes has mainly focused on improving the performance over a wide temperature range through several key approaches including novel solvation engineering for optimising ion transport, addition of flame-retardant additives for enhancing safety, and ion hybridisation strategies for improving the electrochemical stability. These modifications synergistically lead to improved ionic conductivity, redox kinetics and compatibility of electrode-electrolyte interface. Two important directions of further development have emerged. The first is that the precise control of desolvation process, including acceleration and inhibition, is the fundamental method to solve the low-temperature performance bottleneck. Second, perfluorinated electrolytes are very promising due to their intrinsic antioxidant properties and the suppression of parasitic reactions. Their special property to form stable passivation layers on the electrodes significantly improves the cycling stability under

harsh temperature conditions and therefore they are particularly well suited for applications with broad operational temperature windows. These advances represent a progressive move to next-generation electrolyte systems that can improve several performance parameters, including conductivity, safety and temperature tolerance, simultaneously. Further studies are warranted for exploring the synergistic effects of these modification strategies for developing optimal electrolyte formulations for diverse battery applications.

(2) Organic electrode materials are promising candidates for next generation energy storage systems, which have better environmental compatibility, sustainable resource availability, and excellent molecular design flexibility compared to conventional transition metal oxides. The structural flexibility of these materials allows the exact molecular design of a wide range of redox-active compounds including n-type, p-type, and bipolar-type organic molecules, significantly broadening their application from traditional rocking-chair batteries to new DIB systems. In particular, organic compounds of bipolar type, such as phthalocyanine derivatives, exhibit impressive electrochemical versatility due to their extended π-conjugated systems that facilitate simultaneous storage of cation and anion with efficient charge transfer kinetics. However, it is still challenging to use small-molecule organic electrodes, including phthalocyanine-based materials, because they tend to dissolve in aprotic electrolytes, causing severe capacity fading during cycling. Recent advances in polymer chemistry suggest that the construction of conjugated microporous polymer networks, enabling significant improvement of material stability without loss of redox activity, could be a promising solution to this limitation. Several critical research directions should be prioritised to further advance this field: (a) structure of molecules optimisation: development of new organic/polymeric frameworks with enhanced electrolyte resistance and optimised redox characteristics; (b) hybrid material design: integration of bipolar organic compounds with conductive supporting matrices to improve both charge storage capacity and long-term cycling performance; (c) manufacturing process development: development of scalable and cost-effective synthesis routes for high-performance organic electrode materials. Through the strategic combination of these approaches, organic-based DIB systems could overcome current limitations and, over time, mature into viable, sustainable alternatives for large-scale energy storage applications. The inherent benefits of organic materials, coupled with innovative solutions to their solubility problems, make them especially promising candidates for future EES technologies.

(3) A systematic evaluation under abuse conditions is an essential requirement for DIB development. Generally, batteries work best under normal environmental conditions, but they are limited in their operation by very low or very high temperatures, mainly due to limitations related to the electrolyte. High LUMO and low HOMO energy levels are crucial to avoid decomposition and parasitic reactions for the electrolyte stability in high-temperature environments. In contrast, the low-temperature performance depends on the ionic conductivity and the fluidity which are both strongly related to the molecular arrangement of the electrolyte. An ideal electrolyte should enable the formation of a robust and conductive SEI that is thermally stable at subzero temperatures and resistant to excessive growth or degradation under thermal stress. At higher temperature, conventional LIB cathodes undergo incomplete redox reactions, causing transition metal dissolution. These dissolved species migrate to the anode where they destabilise the interface, increase impedance and accelerate capacity fading. Moreover, the decomposition of inorganic SEI components and the catalytic effect of dissolved metals on the solvent degradation result in unstable byproducts like Li_2O and HF. Instead, DIBs use graphite or carbon-based cathodes to avoid transition metal redox reactions, which leads to better cathode stability. The unique solvation dynamics of anions (weak interactions or repulsion with solvent molecules) enables DIBs to exhibit better performance at low temperatures due to the reduction of the energy barriers for solvation/desolvation at the electrode-electrolyte interface. Experimental evidence suggests that anion-hosting cathodes perform better than LIBs in cryogenic conditions. DIBs provide a wider operating temperature range but still have persistent challenges of limited energy density, interfacial instability, electrolyte decomposition, sluggish kinetics and safety risks in extreme or fluctuating temperatures. These challenges are addressed by new strategies including desolvation-free electrode design, solvation structure optimisation, conductivity enhancement, flame-retardant additives, interfacial chemistry modulation, electropolymerization techniques, and advanced intrinsic/extrinsic structural engineering. Future research should focus on designing multifunctional electrolytes and electrode materials that can synergistically solve these challenges to unlock the entire potential of DIBs for next-generation energy storage applications.

(4) The rapid growth of the LIB market will inevitably result in a large volume of spent batteries, which raises critical environmental and resource sustainability issues. LIBs improper disposal can cause leakage of heavy metals, organic electrolytes and graphite anodes, causing soil acidification, organic pollution and loss of valuable materials. Graphite makes up 21% of the total mass of the battery, but current recycling efforts focus

on the high-value metals, leaving graphite largely untapped. With the anticipated increase of LIB waste, effective strategies for the recovery and reuse of graphite are essential to mitigate the environmental risks and promote a circular economy. Recycled graphite from spent LIBs retains a well-preserved layered structure, which will be a promising candidate for energy storage applications. Leaching and thermal treatment can effectively remove the main contaminants, organic binders and residual metals. However, conventional high-temperature calcination (>2000 °C) guarantees high-purity graphite, but is energy-intensive. It causes 15–25% mass loss, which results in a significant decrease in the recovery efficiency. It is thus crucial to develop cost-effective and sustainable graphite recycling strategies to maximise the use of the material. Apart from their traditional application as anode materials, the recycled graphite also shows great potential for application as high-performance cathode materials for DIBs. Different from traditional LIBs, DIBs take advantage of the anion intercalation property of graphite, which provides advantages of higher thermal stability, less transition metal dissolution and better low temperature performance. The recycling of graphite as a cathode can help to solve the capacity fading and interfacial degradation issues typically observed in LIBs at extreme temperatures because DIBs do not undergo redox reactions with transition metals (e.g., Co, Ni, Mn). Besides, the weak solvation interaction of anions and solvent molecules also helps the improved kinetics at low temperature, which further improves the feasibility of the recycled graphite in DIB applications.

To summarise, DIB technology is promising for sustainable large-scale energy storage applications, but further improvements of energy density, cycling stability and safety performance are required.

Author Contributions

H.Z.: data curation, writing—original draft preparation; F.A.: conceptualization; A.K.: investigation; X.X.: reviewing and editing; L.X.: writing, reviewing and editing; R.C.: supervision; L.L.: supervision. All authors have read and agreed to the published version of the manuscript. All authors have read and agreed to the published version of the manuscript.

Funding

This work was supported by the State Key Program of National Natural Science of China (52534010), the National Natural Science Foundation of China (52374410), the National Natural Science Foundation of China (52554002), and Yunnan Fundamental Research Projects (grant Nos. 202401BE070001-049 and 202601CF070026).

Conflicts of Interest

The authors declare no conflict of interest.

Use of AI and AI-Assisted Technologies

No AI tools were utilized for this paper.

References

1. Granados-Moreno, M.; Cid, R.; Arnaiz, M.; et al. How Does $Li_2C_4O_4$ Prelithiation Additive Influence the Solid Electrolyte Interphase of Dual Carbon Lithium-Ion Capacitors? *ACS Appl. Mater. Interfaces* **2024**, *16*, 61846–61857. https://doi.org/10.1021/acsami.4c09411.
2. Li, K.; Hu, X.; Zhang, Z.; et al. Three-dimensional Porous Biogenic Si/C Composite for High Performance Lithium-ion Battery Anode Derived from Equisetum Fluviatile. *J. Inorg. Mater.* **2021**, *36*, 929. https://doi.org/10.15541/jim20200525.
3. Li, S.; Che, Y.; Song, J.; et al. Electrolytic Preparation of Zirconium Metal from a Consumable Zirconium Oxycarbide Anode. *Metall. Mater. Trans. B* **2021**, *52*, 3276–3287. https://doi.org/10.1007/s11663-021-02255-x.
4. Liang, F.; Watanabe, T.; Hayashi, K.; et al. Liquid exfoliation graphene sheets as catalysts for hybrid sodium-air cells. *Mater. Lett.* **2017**, *187*, 32–35. https://doi.org/10.1016/j.matlet.2016.10.054.
5. Chen, K.; Yang, H.; Liang, F.; et al. Microwave-Irradiation-Assisted Combustion toward Modified Graphite as Lithium Ion Battery Anode. *ACS Appl. Mater. Interfaces* **2018**, *10*, 909–914. https://doi.org/10.1021/acsami.7b16418.
6. He, Z.; Li, H.; Ji, W.; et al. Investigation on Li-plating prevention optimal charging protocol of nickel-rich/graphite-SiOx lithium ion battery. *J. Power Sources* **2023**, *571*, 233044. https://doi.org/10.1016/j.jpowsour.2023.233044.
7. Huang, S.; Feng, D.; Zhu, Y.; et al. Enhanced electrochemical performance of NiSbS/NiSb/NiS nanocomposites anchored on graphite nanosheets for sodium-ion battery applications. *J. Mater. Chem. A* **2025**, *13*, 604–616. https://doi.org/10.1039/d4ta07323a.

8. Chong, S.; Qiao, S.; Wang, Z.; et al. Tuning the electrochemical kinetics of bismuth-based conversion-alloying anodes with anion modulation for sodium-ion storage. *Nano Energy* **2024**, *130*, 110097. https://doi.org/10.1016/j.nanoen.2024.110097.
9. Chen, T.; Zhang, A.; Li, X.; et al. Synergistic Construction of Electrode-Electrolyte Interphases via Electrolyte Cosolvent and Additive Chemistry toward Ultrastable and Fast-Charging Li-Rich Batteries. *ACS Appl. Mater. Interfaces* **2025**, *17*, 18359–18370. https://doi.org/10.1021/acsami.4c23006.
10. Zhu, H.; Li, W.; Sun, L. Application of graphite-derived materials in metal-ion batteries. *J. Energy Storage* **2024**, *102*, 114095. https://doi.org/10.1016/j.est.2024.114095.
11. Liu, X.; Pan, Q.; Fan, Y.; et al. Beyond room temperature: Challenges and strategies for wide-temperature dual-ion batteries. *Chem. Eng. J.* **2025**, *520*, 166013.
12. Bamberg, M.; Fuhrmann, F.; Eckert, M.; et al. Insights into self-discharge processes of Al-graphite batteries. *Electrochim. Acta* **2024**, *488*, 144198. https://doi.org/10.1016/j.electacta.2024.144198.
13. International Energy Agency. Global Critical Minerals Outlook 2026. Available online: https://www.iea.org/reports/global-critical-minerals-outlook-2026 (accessed on 16 July 2026).
14. Gavilán-Arriazu, E.M.; Pinto, O.A.; López de Mishima, B.A.; et al. The kinetic origin of the Daumas-Hérold model for the Li-ion/graphite intercalation system. *Electrochem. Commun.* **2018**, *93*, 133–137. https://doi.org/10.1016/j.elecom.2018.07.004.
15. McCullough, F.P.; Levine, A.C.; Snelgrove, R.V. Secondary Battery. U.S. Patent 4,830,938, 16 May 1989.
16. Seel, J.A.; Dahn, J.R. Electrochemical Intercalation of PF_6 into Graphite. *J. Electrochem. Soc.* **2000**, *147*, 892. https://doi.org/10.1149/1.1393288.
17. Placke, T.; Fromm, O.; Lux, S.F.; et al. Reversible Intercalation of Bis(trifluoromethanesulfonyl)imide Anions from an Ionic Liquid Electrolyte into Graphite for High Performance Dual-Ion Cells. *J. Electrochem. Soc.* **2012**, *159*, A1755–A1765. https://doi.org/10.1149/2.011211jes.
18. Ji, B.; Zhang, F.; Song, X.; et al. A Novel Potassium-Ion-Based Dual-Ion Battery. *Adv. Mater.* **2017**, *29*, 1700519. https://doi.org/10.1002/adma.201700519.
19. Holoubek, J.; Yin, Y.; Li, M.; et al. Exploiting Mechanistic Solvation Kinetics for Dual-Graphite Batteries with High Power Output at Extremely Low Temperature. *Angew. Chem. Int. Ed.* **2019**, *58*, 18892–18897. https://doi.org/10.1002/anie.201912167.
20. Zhu, H.; Zhang, F.; Li, J.; et al. Penne-Like MoS_2/Carbon Nanocomposite as Anode for Sodium-Ion-Based Dual-Ion Battery. *Small* **2018**, *14*, 1703951. https://doi.org/10.1002/smll.201703951.
21. Chen, Z.; Yang, C.; Zhang, D.; et al. Mechanistic insight into laser-enhanced LiMn2O4/Zn electrodes for aqueous dual-ion batteries. *J. Energy Storage* **2026**, *162*, 122010. https://doi.org/10.1016/j.est.2026.122010.
22. Yu, D.; Zhu, Q.; Cheng, L.; et al. Anion Solvation Regulation Enables Long Cycle Stability of Graphite Cathodes. *ACS Energy Lett.* **2021**, *6*, 949–958. https://doi.org/10.1021/acsenergylett.1c00043.
23. Xu, Y.; Feng, J.; Ma, H.; et al. Superior Volumetric Capability Dual-Ion Batteries Enabled by A Microsize Niobium Tungsten Oxide Anode. *Adv. Funct. Mater.* **2022**, *32*, 2112223. https://doi.org/10.1002/adfm.202112223.
24. Chen, C.; Wang, J.; Dong, H.; et al. Facile Synthesis of Graphite-Like Carbon Nitride/Zinc Oxide Heterojunction for Microwave Absorption. *J. Alloys Compd.* **2023**, *935*, 167723. https://doi.org/10.1016/j.jallcom.2022.167723.
25. Guo, Y.; Liu, K.; Li, X.; et al. N/P co-doping regulates the local microcrystalline structure of hard carbon to facilitate sodium-ion storage. *J. Mater. Chem. A* **2025**, *13*, 21808–21818. https://doi.org/10.1039/d5ta02023a.
26. Hao, Z.; Zhang, H.; Ruan, Z.; et al. Tuning the Electronic Properties of Atomically Precise Graphene Nanoribbons by Bottom-Up Fabrication. *ChemNanoMat* **2020**, *6*, 493–515. https://doi.org/10.1002/cnma.201900706.
27. Jin, L.; Wu, H. Carbon sphere-based hierarchical architecture for electrode materials: The role of copolymer composition and pyrolysis temperature. *J. Mater. Sci.* **2019**, *54*, 8226–8235. https://doi.org/10.1007/s10853-019-03501-z.
28. Zhang, L.; Wang, H.; Zhang, X.; et al. A Review of Emerging Dual-Ion Batteries: Fundamentals and Recent Advances. *Adv. Funct. Mater.* **2021**, *31*, 2010958. https://doi.org/10.1002/adfm.202010958.
29. Eidenschink, J.; Matysik, F.M. Simultaneous Scanning Ion Conductance and Electrochemical Microscopy in Lithium-Ion Battery Research. *ChemElectroChem* **2024**, *11*, e202300577. https://doi.org/10.1002/celc.202300577.
30. Ding, J.; Huang, Y.; Cheng, W.; et al. Boosting ion diffusion kinetics of Fe_2O_3/MoC@NG via heterointerface engineering and pseudocapacitance behavior: An alternative high-rate anode for high-capacity lithium dual-ion batteries. *Chem. Eng. J.* **2024**, *481*, 148499. https://doi.org/10.1016/j.cej.2023.148499.
31. Ou, X.; Gong, D.; Han, C.; et al. Advances and Prospects of Dual-Ion Batteries. *Adv. Energy Mater.* **2021**, *11*, 2102498. https://doi.org/10.1002/aenm.202102498.
32. Holoubek, J.; Chen, Z.; Liu, P. Application-Based Prospects for Dual-Ion Batteries. *ChemSusChem* **2023**, *16*, e202201245. https://doi.org/10.1002/cssc.202201245.
33. Sandstrom, S.K.; Chen, X.; Ji, X. A review of halide charge carriers for rocking-chair and dual-ion batteries. *Carbon Energy* **2021**, *3*, 627–653. https://doi.org/10.1002/cey2.110.

34. Qiu, X.; Liu, H.; Duan, Y.; et al. Designing High-Performance Dual-Ion Batteries: Insights into Electrode, Electrolyte, and Interface Engineering. *Adv. Energy Mater.* **2025**, *15*, 2501016. https://doi.org/10.1002/aenm.202501016.
35. Sui, Y.; Liu, C.; Masse, R.C.; et al. Dual-ion batteries: The emerging alternative rechargeable batteries. *Energy Storage Mater.* **2020**, *25*, 1–32. https://doi.org/10.1016/j.ensm.2019.11.003.
36. Placke, T.; Heckmann, A.; Schmuch, R.; et al. Perspective on Performance, Cost, and Technical Challenges for Practical Dual-Ion Batteries. *Joule* **2018**, *2*, 2528–2550. https://doi.org/10.1016/j.joule.2018.09.003.
37. Wang, H.G.; Li, Q.; Wu, Q.; et al. Conjugated Microporous Polymers with Bipolar and Double Redox-Active Centers for High-Performance Dual-Ion, Organic Symmetric Battery. *Adv. Energy Mater.* **2021**, *11*, 2100381. https://doi.org/10.1002/aenm.202100381.
38. Jacob, M.S.; Ramireddy, T.; Glushenkov, A.M. Alloying-type anode materials for dual-ion batteries: An inceptive review. *J. Mater. Chem. A* **2026**, *14*, 11221–11242. https://doi.org/10.1039/d5ta08606j.
39. Zhou, H.; Shi, Y.; Zhou, H.; et al. Synergistic interface engineering of stable zinc anode and anti-shuttle separator for high-performance zinc-based dual-ion batteries. *J. Power Sources* **2026**, *671*, 239481. https://doi.org/10.1016/j.jpowsour.2026.239481.
40. Tang, Z.; Xu, L.; Wang, Z.; et al. Effect of Microwave-Activated Sintering on Microstructure and Properties of Graphite/Copper Composites. *ACS Appl. Electron. Mater.* **2021**, *3*, 2268–2276. https://doi.org/10.1021/acsaelm.1c00188.
41. Sun, Z.; Zhu, K.; Liu, P.; et al. Optimized Cathode for High-Energy Sodium-Ion Based Dual-Ion Full Battery with Fast Kinetics. *Adv. Funct. Mater.* **2021**, *31*, 2107830. https://doi.org/10.1002/adfm.202107830.
42. Inamoto, J.; Enoki, S.; Inoo, A.; et al. Promise of dual carbon batteries with graphene-like graphite as both electrodes. *Carbon* **2024**, *216*, 118512. https://doi.org/10.1016/j.carbon.2023.118512.
43. Xie, S.; Chen, Y.; Xie, Y.; et al. Unlocking High-Capacity Graphite Cathode in Dual-Ion Batteries Through Structural Disorder Regulation. *Adv. Funct. Mater.* **2026**, *36*, e29373. https://doi.org/10.1002/adfm.202529373.
44. Han, X.; Jiang, H.; Mu, P.; et al. Helmholtz Plane Regulation Empowers PF_6^-Permselectivity Towards High Coulombic Efficiency Dual Ion Battery of 5.5 V. *Angew. Chem. Int. Ed.* **2025**, *64*, e202412753. https://doi.org/10.1002/anie.202412753.
45. Gu, Y.; Li, W.; Zheng, Y.; et al. Nitrogen-Centered Redox Active Polymers with Extended π-Conjugated Structures for High-Performance Potassium Dual-Ion Batteries. *ACS Sustain. Chem. Eng.* **2025**, *13*, 16694–16703. https://doi.org/10.1021/acssuschemeng.5c07991.
46. Liu, X.; Zhang, Y.; Zhou, C.; et al. A large π-conjugated p-type small molecule towards practical Li-dual-ion batteries. *Energy Storage Mater.* **2026**, *84*, 104795. https://doi.org/10.1016/j.ensm.2025.104795.
47. Guo, M.; Li, W.; Tang, W.; et al. A p-type small-molecule organic cathode simultaneously for high-voltage Li/Na-based dual-ion full batteries. *Energy Storage Mater.* **2025**, *74*, 103979. https://doi.org/10.1016/j.ensm.2024.103979.
48. Zhang, Y.; Li, X.; Fu, Y.; et al. Organophosphine-Functionalized Nitrogen-Rich Porous p-Type Polymer Electrode for Li-Dual-Ion Batteries. *Adv. Funct. Mater.* **2026**, *36*, e00020. https://doi.org/10.1002/adfm.202600020.
49. Wu, H.; Luo, S.; Wang, H.; et al. An ultra-stable sodium dual-ion battery based on S/Se co-doped covalent organic framework anode with 12,000 cycles under lean electrolyte. *Energy Storage Mater.* **2025**, *75*, 104052. https://doi.org/10.1016/j.ensm.2025.104052.
50. Liu, S.; Ke, X.; Zhou, Y.; et al. A new long-cycle mechanism based on p-type@n-type organic composite anode material for dual-ion battery. *J. Energy Storage* **2025**, *132*, 117755. https://doi.org/10.1016/j.est.2025.117755.
51. Li, Y.; Tan, C.; Ding, R.; et al. Designing a pseudocapacitive binary Zn/Mn perovskite fluoride anode with a conversion/alloying/insertion hybrid mechanism for advanced Na-ion capacitors and Na-based dual ion batteries. *Nanoscale* **2025**, *17*, 21468–21474. https://doi.org/10.1039/d5nr03023d.
52. Ma, X.; Liu, X.; Liu, G.; et al. Superior dual-ion batteries enabled by mildly expanded graphite cathode and hierarchical MoS_2@C anode. *Electrochim. Acta* **2024**, *474*, 143568. https://doi.org/10.1016/j.electacta.2023.143568.
53. Rong, J.; Yu, X.; Fan, Z.; et al. Nanostructure of mesophase pitch-based graphite in the matrix of C/C composite. *Mater. Lett.* **2019**, *234*, 364–367. https://doi.org/10.1016/j.matlet.2018.09.143.
54. Shen, L.; Li, S.; Wang, Y.; et al. Upcycling Photovoltaic Silicon Waste Into Cost-Effectiveness Si/C Anode Materials. *Carbon Energy* **2025**, *7*, e70004. https://doi.org/10.1002/cey2.70004.
55. Wang, L.; Jiang, Y.; Li, S.Y.; et al. Scalable synthesis of N-doped Si/G@voids@C with porous structures for high-performance anode of lithium-ion batteries. *Rare Met.* **2023**, *42*, 4091–4102. https://doi.org/10.1007/s12598-023-02472-0.
56. Yuan, W.; Ding, T.; Mou, P.; et al. Semi-Solid CNT@NaK Anode for Potassium Metal Battery. *Adv. Funct. Mater.* **2023**, *33*, 2209774. https://doi.org/10.1002/adfm.202209774.
57. Zhang, Z.; Xi, F.; Li, S.; et al. High-performance Si/nano-Cu/CNTs/C anode derived from photovoltaic silicon waste: A potential photovoltaic-energy storage strategy. *Mater. Today Energy* **2021**, *20*, 100671. https://doi.org/10.1016/j.mtener.2021.100671.

58. Yu, F.; Chen, X.; Huang, J.; et al. Molecular size matching of dopant in polypyrrole and anion in dual-ion battery enhancing the energy storage ability and dynamics of polypyrrole cathode. *Chem. Eng. J.* **2025**, *510*, 161471. https://doi.org/10.1016/j.cej.2025.161471.
59. Tang, B.; Zhang, Y.; Ji, B.; et al. Ion-Mediated Carbon Microdomain Engineering Boosting Enhanced Plateau Capacity of Carbon Anode under High Rate Towards High-Performance Sodium Dual-Ion Batteries. *Nano-Micro Lett.* **2026**, *18*, 161. https://doi.org/10.1007/s40820-025-02008-4.
60. Yoo, J.H.; Kim, H.; Jo, H.; et al. Transforming waste anthracite-to-energy, mesoporous anode for lithium dual-ion batteries based on the position control of SiC and SiO_2. *J. Energy Storage* **2026**, *144*, 119738. https://doi.org/10.1016/j.est.2025.119738.
61. Wang, X.; Liu, Y.; Li, J.; et al. Phenazinyl polymer@rGO composite cathode materials with fast charging and wide temperature adaptability for sodium dual-ion batteries. *Electrochim. Acta* **2025**, *526*, 146161. https://doi.org/10.1016/j.electacta.2025.146161.
62. Asenbauer, J.; Eisenmann, T.; Kuenzel, M.; et al. The success story of graphite as a lithium-ion anode material—fundamentals, remaining challenges, and recent developments including silicon (oxide) composites. *Sustain. Energy Fuels* **2020**, *4*, 5387–5416. https://doi.org/10.1039/d0se00175a.
63. Read, J.A. *In-Situ* Studies on the Electrochemical Intercalation of Hexafluorophosphate Anion in Graphite with Selective Cointercalation of Solvent. *J. Phys. Chem. C* **2015**, *119*, 8438–8446. https://doi.org/10.1021/jp5115465.
64. Fu, Y.; Li, W.; Gu, Y.; et al. Dual-Redox Active Sites Enable High Initial Coulombic Efficiency and Long Lifespan of Carbazole-Based Cathodes for Lithium Dual-Ion Batteries. *Adv. Funct. Mater.* **2026**, *36*, e23278. https://doi.org/10.1002/adfm.202523278.
65. Tang, H.; Jiang, J.; Guo, H.; et al. Biphenylite with an Ultrahigh Capacity of Hexafluorophosphate Anions as a Promising Electrode Material in Dual-Ion Batteries. *ACS Appl. Mater. Interfaces* **2025**, *17*, 52202–52211. https://doi.org/10.1021/acsami.5c12471.
66. Heckmann, A.; Fromm, O.; Rodehorst, U.; et al. New insights into electrochemical anion intercalation into carbonaceous materials for dual-ion batteries: Impact of the graphitization degree. *Carbon* **2018**, *131*, 201–212. https://doi.org/10.1016/j.carbon.2018.01.099.
67. Wang, M.; Tang, Y. A Review on the Features and Progress of Dual-Ion Batteries. *Adv. Energy Mater.* **2018**, *8*, 1703320. https://doi.org/10.1002/aenm.201703320.
68. Zhao, Y.M.; Yue, F.S.; Li, S.C.; et al. Advances of polymer binders for silicon-based anodes in high energy density lithium-ion batteries. *InfoMat* **2021**, *3*, 460–501. https://doi.org/10.1002/inf2.12185.
69. Zhang, Y.; Cao, X.; Xiao, P. Tuning electrolyte solvation structure with Co-solvent engineering to enable highly reversible and stable Zn-graphite dual-ion batteries. *J. Power Sources* **2024**, *590*, 233805. https://doi.org/10.1016/j.jpowsour.2023.233805.
70. Chen, N.; Wang, B.; Mei, W.; et al. Improved performance of dual-ion battery by tailoring the solvation of anion using trace sulfolane. *J. Energy Storage* **2025**, *123*, 116770. https://doi.org/10.1016/j.est.2025.116770.
71. Guo, Q.; Kim, K.I.; Jiang, H.; et al. A High-Potential Anion-Insertion Carbon Cathode for Aqueous Zinc Dual-Ion Battery. *Adv. Funct. Mater.* **2020**, *30*, 2002825. https://doi.org/10.1002/adfm.202002825.
72. Yong, K.; Fang, H.; Wang, B.; et al. Synergistic Structural Engineering of Tunnel-Type Polyantimonic Acid Enables Dual-Boosted Volumetric and Areal Lithium Energy Storage. *Adv. Energy Mater.* **2022**, *12*, 2200653. https://doi.org/10.1002/aenm.202200653.
73. Zhao, C.; Fang, B.; Wang, R.; et al. Structure engineering and heteroatom doping-enabled high-energy and fast-charging dual-ion batteries. *Chem. Eng. J.* **2024**, *490*, 151537. https://doi.org/10.1016/j.cej.2024.151537.
74. Kim, K.I.; Guo, Q.; Tang, L.; et al. Reversible Insertion of Mg-Cl Superhalides in Graphite as a Cathode for Aqueous Dual-Ion Batteries. *Angew. Chem. Int. Ed.* **2020**, *59*, 19924–19928. https://doi.org/10.1002/anie.202009172.
75. Sun, Z.; Jiang, H.; Liu, P.; et al. Pre-Activated Cascade Redox Enables High-Voltage Multi-Electron Anion Storage in Graphite. *Angew. Chem. Int. Ed.* **2026**, *65*, e5529195. https://doi.org/10.1002/anie.5529195.
76. He, Y.; Shen, X.; Červenka, J. In Situ Modification of Sulfur-Based Cathode Electrolyte Interphases for Boosting Zinc/Graphite Dual-Ion Batteries via Vinylene Carbonate Additive and Dipropylene Glycol Methyl Ether/Water Mixed Solvent. *ACS Sustain. Chem. Eng.* **2025**, *13*, 8363–8372. https://doi.org/10.1021/acssuschemeng.5c01897.
77. Luo, W.; Yu, D.; Ge, T.; et al. Balancing salt concentration and fluorinated cosolvent for graphite cathode-based dual-ion batteries. *Appl. Energy* **2024**, *358*, 122652. https://doi.org/10.1016/j.apenergy.2024.122652.
78. Zheng, Y.; Zhang, W.; Liu, F.; et al. Additive-rejuvenated anions (De)intercalation into graphite cathode enables optimum dual-ion battery. *Energy Storage Mater.* **2024**, *67*, 103326. https://doi.org/10.1016/j.ensm.2024.103326.
79. Zhang, K.; Yu, Q.; Sun, J.; et al. Halogen Electrochemistry Enabled Complementary Lithium/Halogen Dual-Ion Batteries with Enhanced Capacity and Cyclability. *Nano Lett.* **2025**, *25*, 16554–16563. https://doi.org/10.1021/acs.nanolett.5c04968.

80. Yang, H.; Liu, F.; Jiang, Z.; et al. Constructing a 5.2 V High-Voltage Electrolyte via TMSB Additive Enables Ultrahigh Rate Performance Graphite-Based Dual-Ion Batteries. *Nano Lett.* **2025**, *25*, 8511–8518. https://doi.org/10.1021/acs.nanolett.5c00896.
81. Hu, X.; Sun, W.; Zhou, A.; et al. Anion Redistribution in Solvation Structure Enables a Stable Graphite Cathode in Dual-Ion Batteries. *ACS Nano* **2025**, *19*, 18686–18697. https://doi.org/10.1021/acsnano.5c03112.
82. Cheng, Z.; Guo, L.; Dong, Q.; et al. Highly Durable and Ultrafast Cycling of Dual-Ion Batteries via *In Situ* Construction of Cathode-Electrolyte Interphase. *Adv. Energy Mater.* **2022**, *12*, 2202253. https://doi.org/10.1002/aenm.202202253.
83. Wang, S.; Guan, Y.; Gan, F.; et al. Charge Carriers for Aqueous Dual-Ion Batteries. *ChemSusChem* **2023**, *16*, e202201373. https://doi.org/10.1002/cssc.202201373.
84. Zhou, W.; Sit, P.H.L. First-Principles Understanding of the Staging Properties of the Graphite Intercalation Compounds towards Dual-Ion Battery Applications. *ACS Omega* **2020**, *5*, 18289–18300. https://doi.org/10.1021/acsomega.0c01950.
85. Zhang, Y.; Jiang, H.; Du, X.; et al. Solvent's Covert Role: Concerted Anion-Solvent Co-Intercalation Rewrites Voltage Rules for Dual-Ion Batteries. *Angew. Chem. Int. Ed.* **2025**, *64*, e15181. https://doi.org/10.1002/anie.202515181.
86. Xue, Z.; Gao, Z.; Zhao, X. Halogen Storage Electrode Materials for Rechargeable Batteries. *Energy Environ. Mater.* **2022**, *5*, 1155–1179. https://doi.org/10.1002/eem2.12442.
87. Liu, W.; Li, Y.; Yang, H.; et al. Pursuing high voltage and long lifespan for low-cost Al-based rechargeable batteries: Dual-ion design and prospects. *Energy Storage Mater.* **2023**, *62*, 102922. https://doi.org/10.1016/j.ensm.2023.102922.
88. Zhao, Z.; Alshareef, H.N. Sustainable Dual-Ion Batteries beyond Li. *Adv. Mater.* **2024**, *36*, 2309223. https://doi.org/10.1002/adma.202309223.
89. Pi, Y.; Xiao, J.; Liu, Y.; et al. Sustainable recycling of $Na_3V_2(PO_4)_3$ cathodes: A pathway to high-safety Na-Ni dual-ion batteries for scalable energy storage. *J. Energy Storage* **2025**, *113*, 115593. https://doi.org/10.1016/j.est.2025.115593.
90. He, Q.; Guo, C.; Han, K.; et al. Direct recycling of spent graphite anode via calcium silicate coating for high-capacity and fast lithium storage. *Carbon* **2025**, *244*, 120727. https://doi.org/10.1016/j.carbon.2025.120727.
91. Huang, P.; Li, Z.; Chen, L.; et al. Ultrafast Dual-Shock Chemistry Synthesis of Ordered/Disordered Hybrid Carbon Anodes: High-Rate Performance of Li-Ion Batteries. *ACS Nano* **2024**, *18*, 18344–18354. https://doi.org/10.1021/acsnano.4c02300.
92. Gong, D.; Wei, C.; Liang, Z.; et al. Recent Advances on Sodium-Ion Batteries and Sodium Dual-Ion Batteries: State-of-the-Art Na^+ Host Anode Materials. *Small Sci.* **2021**, *1*, 2100014. https://doi.org/10.1002/smsc.202100014.
93. Luo, W.; Zhang, X.; Cai, H.; et al. A high-energy asynchronously reverse dual-ion battery based on H^-/Na^+ insertion chemistry. *Energy Environ. Sci.* **2026**, *19*, 926–938. https://doi.org/10.1039/d5ee06051f.
94. Li, J.G.; Mu, J.J.; Liu, Z.M.; et al. Boosting potassium-based dual ion battery with high energy density and long lifespan by red phosphorous. *J. Power Sources* **2023**, *571*, 233054. https://doi.org/10.1016/j.jpowsour.2023.233054.
95. Zheng, C.; Jian, B.; Xu, X.; et al. Regulating microstructure of walnut shell-derived hard carbon for high rate and long cycling sodium-based dual-ion batteries. *Chem. Eng. J.* **2023**, *455*, 140434. https://doi.org/10.1016/j.cej.2022.140434.
96. Zhang, M.; Shoaib, M.; Fei, H.; et al. Hierarchically Porous N-Doped Carbon Fibers as a Free-Standing Anode for High-Capacity Potassium-Based Dual-Ion Battery. *Adv. Energy Mater.* **2019**, *9*, 1901663. https://doi.org/10.1002/aenm.201901663.
97. Yu, A.; Pan, Q.; Zhang, M.; et al. Fast Rate and Long Life Potassium-Ion Based Dual-Ion Battery through 3D Porous Organic Negative Electrode. *Adv. Funct. Mater.* **2020**, *30*, 2001440. https://doi.org/10.1002/adfm.202001440.
98. Wang, Z.; Xu, Y.; Xu, S.; et al. The cation effect on halogen intercalation into graphite electrode in aqueous zinc dual-ion batteries. *Electrochim. Acta* **2026**, *548*, 147992. https://doi.org/10.1016/j.electacta.2025.147992.
99. Zhou, X.; Liu, Q.; Jiang, C.; et al. Strategies towards Low-Cost Dual-Ion Batteries with High Performance. *Angew. Chem. Int. Ed.* **2020**, *59*, 3802–3832. https://doi.org/10.1002/anie.201814294.
100. Shi, H.; Guo, F.; Lv, A.; et al. DDQ/graphite dual-ion hybrid positive electrode in new AMC/$AlCl_3$ electrolyte for advanced aluminum-organic battery. *Chem. Eng. J.* **2023**, *470*, 144253. https://doi.org/10.1016/j.cej.2023.144253.
101. Liu, X.; Ma, X.; Zhang, X.; et al. Insertion of $AlCl_3$ in graphite as both cation and anion insertion host for dual-ion battery. *J. Energy Storage* **2023**, *72*, 108687. https://doi.org/10.1016/j.est.2023.108687.
102. Zhou, R.; Hou, Z.; Fan, K.; et al. An advanced organic cathode for non-aqueous and aqueous calcium-based dual ion batteries. *J. Power Sources* **2023**, *569*, 232995. https://doi.org/10.1016/j.jpowsour.2023.232995.
103. Cai, W.; Zhang, L.; Chen, K.; et al. Recycling of Spent Graphite from Lithium-Ion Batteries for Aqueous Zn Dual-Ion Batteries. *ACS Appl. Mater. Interfaces* **2024**, *16*, 50897–50904. https://doi.org/10.1021/acsami.4c11552.
104. Cai, P.; Chen, K.; Lu, Z.; et al. Aqueous OH^-/H^+ Dual-Ion Zn-Based Batteries. *ChemSusChem* **2023**, *16*, e202201034. https://doi.org/10.1002/cssc.202201034.
105. Tao, S.; Demir, B.; Baktash, A.; et al. Solvent-derived Fluorinated Secondary Interphase for Reversible Zn-graphite Dual-ion Batteries. *Angew. Chem. Int. Ed.* **2023**, *62*, e202307208. https://doi.org/10.1002/anie.202307208.
106. Wang, S.; Yu, Q.; Sun, W.; et al. A glutaronitrile single-solvent triple-salt electrolyte enables high-voltage and long-cycling lithium-ion batteries. *Electrochim. Acta* **2025**, *540*, 147209. https://doi.org/10.1016/j.electacta.2025.147209.

107. Read, J.A.; Cresce, A.V.; Ervin, M.H.; et al. Dual-graphite chemistry enabled by a high voltage electrolyte. *Energy Environ. Sci.* **2014**, *7*, 617–620. https://doi.org/10.1039/c3ee43333a.
108. Vu, M.C.; Srinivasan, H.S.; Mirmira, P.; et al. A transition-metal-and-solvent-free dual-graphite battery. *J. Mater. Chem. A* **2026**, *14*, 31889–31903. https://doi.org/10.1039/d6ta00159a.
109. Fan, H.; Qi, L.; Wang, H. Intercalation Behavior of Hexafluorophosphate into Graphite Electrode from Propylene/ Ethylmethyl Carbonates. *J. Electrochem. Soc.* **2017**, *164*, A2262–A2267. https://doi.org/10.1149/2.0371712jes.
110. Fan, H.; Gao, J.; Qi, L.; et al. Hexafluorophosphate anion intercalation into graphite electrode from sulfolane/ethylmethyl carbonate solutions. *Electrochim. Acta* **2016**, *189*, 9–15. https://doi.org/10.1016/j.electacta.2015.12.078.
111. Akella, S.H.; Sham Lal, M.; Kumar, Y.; et al. Improved Electrochemical Properties of Nickel-Rich, Low-Cobalt Layered Oxide Cathodes Using Dual-Functional Di-*tert*-butylmethyl Adamantoyl Silane Additives. *ACS Appl. Energy Mater.* **2024**, *7*, 2039–2047. https://doi.org/10.1021/acsaem.3c03273.
112. Guan, S.; Peng, Q.; Guo, X.; et al. A review of the advances and prospects of aqueous Dual-Ion batteries. *Chem. Eng. J.* **2024**, *493*, 152864. https://doi.org/10.1016/j.cej.2024.152864.
113. Huang, Z.; Hou, Y.; Wang, T.; et al. Manipulating anion intercalation enables a high-voltage aqueous dual ion battery. *Nat. Commun.* **2021**, *12*, 3106. https://doi.org/10.1038/s41467-021-23369-5. Correction in *Nat. Commun.* **2021**, *12*, 4885.
114. Yang, D.; Watanabe, M.; Inada, M.; et al. Tracking side chain-reactions in aqueous dual-ion batteries to reveal multifactorial self-discharge mechanism. *Energy Storage Mater.* **2025**, *80*, 104382. https://doi.org/10.1016/j.ensm.2025.104382.
115. Wrogemann, J.M.; Künne, S.; Heckmann, A.; et al. Development of Safe and Sustainable Dual-Ion Batteries Through Hybrid Aqueous/Nonaqueous Electrolytes. *Adv. Energy Mater.* **2020**, *10*, 1902709. https://doi.org/10.1002/aenm.201902709.
116. Asfaw, H.D.; Kotronia, A.; Garcia-Araez, N.; et al. Charting the course to solid-state dual-ion batteries. *Carbon Energy* **2024**, *6*, e425. https://doi.org/10.1002/cey2.425.
117. Xu, W.; Li, L.; Zhao, Y.; et al. Some basics and details for better dual-ion batteries. *Energy Environ. Sci.* **2025**, *18*, 2686–2719. https://doi.org/10.1039/d4ee04063e.
118. Pan, H.; Gu, X.; Lv, X.; et al. Rapid anion transporting and mechanically robust cathode-electrolyte interphase for ultrafast and highly reversible dual-ion batteries within a wide temperature range. *J. Energy Chem.* **2025**, *109*, 100–108. https://doi.org/10.1016/j.jechem.2025.05.045.
119. Zhu, M.; Cheng, W.; Wang, H.; et al. Dual-Salt Chaotropic Eutectic Electrolyte for Enhancing Low-Temperature Zinc-Ion Batteries. *Angew. Chem. Int. Ed.* **2026**, *65*, e18700. https://doi.org/10.1002/anie.202518700.
120. Wang, C.; Oka, S.; Avais, M.; et al. Organic dual-ion batteries with low-temperature operability and structural reinforcement. *J. Mater. Chem. A* **2025**, *13*, 31279–31291. https://doi.org/10.1039/d5ta01626f.
121. Wu, Z.; Duan, J.; Sun, C.; et al. An Imidazole-Based Electrolyte Additive for Enhancing the Cyclability of Graphite||$LiFePO_4$ Batteries. *ACS Appl. Mater. Interfaces* **2025**, *17*, 35372–35381. https://doi.org/10.1021/acsami.5c01749.
122. Zhou, Z.; Li, N.; Yang, Y.; et al. Ultra-Lightweight 3D Carbon Current Collectors: Constructing All-Carbon Electrodes for Stable and High Energy Density Dual-Ion Batteries. *Adv. Energy Mater.* **2018**, *8*, 1801439. https://doi.org/10.1002/ aenm.201801439.
123. Han, C.; Xu, Y.S.; Hu, Z.; et al. Designing High-Performance Dual-Ion Batteries at High-Voltage: Challenges, Strategies, and Prospects. *Nano-Micro Lett.* **2026**, *18*, 339. https://doi.org/10.1007/s40820-026-02114-x.
124. Heidrich, B.; Heckmann, A.; Beltrop, K.; et al. Unravelling charge/discharge and capacity fading mechanisms in dual-graphite battery cells using an electron inventory model. *Energy Storage Mater.* **2019**, *21*, 414–426. https://doi.org/ 10.1016/j.ensm.2019.05.031.
125. Wu, H.; Li, C.; Hua, H.; et al. A comprehensive perspective on emerging dual-ion batteries: From materials and mechanisms to applications. *Prog. Mater. Sci.* **2027**, *165*, 101799. https://doi.org/10.1016/j.pmatsci.2026.101799.
126. Mishra, K.K.; Sanjaykumar, C.; Zubair, M.O.; et al. A water-based binder for improved adhesion and reversibility of the graphite cathode for sodium dual-ion batteries. *Nanoscale* **2026**, *18*, 11837–11848. https://doi.org/10.1039/d5nr04941e.
127. Chen, C.; Lee, C.S.; Tang, Y. Fundamental Understanding and Optimization Strategies for Dual-Ion Batteries: A Review. *Nano-Micro Lett.* **2023**, *15*, 121. https://doi.org/10.1007/s40820-023-01086-6.
128. He, Y.; Dong, Y.; Zhang, Y.; et al. Graphene Nano-Blister in Graphite for Future Cathode in Dual-Ion Batteries: Fundamentals, Advances, and Prospects. *Adv. Sci.* **2023**, *10*, 2207426. https://doi.org/10.1002/advs.202207426.
129. Guo, J.; Wu, H.; Wang, H.; et al. Biomass-Derived N/S Co-Doped Carbon with Integrated Disordered and Ordered Structures for High-Performance Dual-Ion Batteries. *Small* **2026**, *22*, e73548. https://doi.org/10.1002/smll.73548.
130. Guo, H.; Elmanzalawy, M.; Sivakumar, P.; et al. Unifying electrolyte formulation and electrode nanoconfinement design to enable new ion–solvent cointercalation chemistries. *Energy Environ. Sci.* **2024**, *17*, 2100–2116. https://doi.org/ 10.1039/d3ee04350a.
131. Ghosh, S.; Mp, N.; Muduli, S.; et al. Optimizing anion storage performances of graphite/ non-graphitic carbon composites as cathodes for dual-ion batteries. *Electrochim. Acta* **2023**, *441*, 141754. https://doi.org/10.1016/j.electacta.2022.141754.

132. Zhuo, J.; Wang, X.; Sheng, N.; et al. Dual-activation with oyster shell: Synergistic engineering of N/P co-doped hierarchical porous carbon from intumescent flame retardants for high-performance dual-ion batteries. *J. Energy Storage* **2026**, *150*, 120481. https://doi.org/10.1016/j.est.2026.120481.
133. Ghosh, S.; Bhattacharjee, U.; Dutta, J.; et al. Ultrathin, flexible and smooth carbon coating extends the cycle life of dual-ion batteries. *J. Power Sources* **2023**, *584*, 233585. https://doi.org/10.1016/j.jpowsour.2023.233585.
134. Li, F.; Li, Y.; Li, H.; et al. AlF_3-stabilized cathode electrolyte interphase with superior PF_6^- affinity and PF_6^- -transferred characteristics for dual-ion batteries. *Energy Storage Mater.* **2025**, *80*, 104353. https://doi.org/10.1016/j.ensm.2025.104353.
135. Ghosh, S.; Sarma, D.; Mahata, A.; et al. Differences between cation and anion storage electrochemistry of graphite and its impact on dual graphite battery. *J. Power Sources* **2024**, *589*, 233721. https://doi.org/10.1016/j.jpowsour.2023.233721.
136. Yang, J.; Xu, C.; Zhou, Z.; et al. $FeSe_2$ graphite intercalation compounds derived from spent graphite with spatial confinement effect enable high-performance sodium storage. *Chem. Eng. J.* **2026**, *528*, 172573. https://doi.org/10.1016/j.cej.2026.172573.
137. Chen, Y.; Xie, S.; Lao, Y.; et al. Realizing anion/ cation co-storage via forming -C-S-C- bonds in sulfur-doped graphitized carbon for high capacity cathode of dual-ion battery. *Energy Storage Mater.* **2026**, *88*, 105156. https://doi.org/10.1016/j.ensm.2026.105156.
138. Zhang, X.; Yan, W.; Li, J.; et al. Anion Pillars Enable High Energy Density Sodium Dual-Ion Battery with Ultra-Long Cycle Life. *Angew. Chem. Int. Ed.* **2026**, *65*, e21536. https://doi.org/10.1002/anie.202521536.
139. Xie, S.; Jing, P.; Chen, Y.; et al. Upcycling spent graphite via interlayer-force weakening boosts fast and durable anion storage. *Energy Storage Mater.* **2026**, *91*, 105572. https://doi.org/10.1016/j.ensm.2026.105572.
140. He, Y.; Chen, Z.; Zhang, Y. Strategies for improving cathode electrolyte interphase in high-performance dual-ion batteries. *iScience* **2024**, *27*, 110491. https://doi.org/10.1016/j.isci.2024.110491.
141. Liang, J.; Lin, Q.; Rawal, A.; et al. Ionic Conductive Polymer Stabilized Cathode–Electrolyte Interface for Quasi-Solid-State Dual-Ion Battery. *ACS Energy Lett.* **2024**, *9*, 1082–1089. https://doi.org/10.1021/acsenergylett.4c00011.
142. Hu, X.; Ma, Y.; Qu, W.; et al. Large Interlayer Distance and Heteroatom-Doping of Graphite Provide New Insights into the Dual-Ion Storage Mechanism in Dual-Carbon Batteries. *Angew. Chem. Int. Ed.* **2023**, *62*, e202307083. https://doi.org/10.1002/anie.202307083.
143. Kotronia, A.; van Ekeren, W.W.A.; Asfaw, H.D.; et al. Impact of Binders on Self-Discharge in Graphite Dual-Ion Batteries. *Electrochem. Commun.* **2023**, *146*, 107424. https://doi.org/10.1016/j.elecom.2022.107424.
144. Li, F.; Shen, Y.F.; He, B.; et al. PF_6^- and Na^+ Co-Intercalation in Graphite Cathode of Sodium Dual-Ion Batteries by Enhanced Surface Concentration Effect. *ChemSusChem* **2025**, *18*, e202402691. https://doi.org/10.1002/cssc.202402691.
145. Jiang, H.; Chen, Z.; Yang, Y.; et al. Rational Design of Functional Electrolytes Towards Commercial Dual-Ion Batteries. *ChemSusChem* **2023**, *16*, e202201561. https://doi.org/10.1002/cssc.202201561.
146. Sabaghi, D.; Wang, G.; Mikhailova, D.; et al. High energy density and durable pouch-cell graphite-based dual ion battery using concentrated hybrid electrolytes. *J. Power Sources* **2023**, *588*, 233685. https://doi.org/10.1016/j.jpowsour.2023.233685.
147. Supiňková, T.; Zukalová, M.; Kakavas, N.; et al. Electrolyte effects and stability of Zn/Li dual-ion batteries with water-in-salt electrolytes. *J. Power Sources* **2025**, *655*, 237983. https://doi.org/10.1016/j.jpowsour.2025.237983.
148. Lang, Q.; Chen, F.; Zhang, J.; et al. An Energy-Dense Nonmetal Dual-Ion Battery Enabled by Weakly Interacted Ionic Liquid and a Ladder Polymer. *Adv. Funct. Mater.* **2026**, *36*, e29911. https://doi.org/10.1002/adfm.202529911.
149. He, Y.; Yu, F.; Červenka, J. Salt particle suspension electrolyte with trace-water for improving ionic concentrations at interfaces in zinc-based dual-ion batteries. *J. Mater. Chem. A* **2025**, *13*, 15871–15882. https://doi.org/10.1039/d5ta00256g.
150. Patra, D.; Ghosh, S.; Parida, R.; et al. Unlocking higher performance of dual-ion storage via fluorene substitution in bipolar conjugated polymers featuring dual acceptors. *Chem. Eng. J.* **2025**, *524*, 168654. https://doi.org/10.1016/j.cej.2025.168654.
151. Kotronia, A.; Asfaw, H.D.; Edström, K. Evaluating electrolyte additives in dual-ion batteries: Overcoming common pitfalls. *Electrochim. Acta* **2023**, *459*, 142517. https://doi.org/10.1016/j.electacta.2023.142517.
152. Chen, S.; Huang, L.; Liang, J.; et al. Single fluorosilane ester additive for F/Si-enriched inorganic interphases enabling durable high-voltage graphite/$LiCoO_2$ pouch cells. *Energy Storage Mater.* **2025**, *81*, 104501. https://doi.org/10.1016/j.ensm.2025.104501.
153. Xu, Z.; Huang, R.; Huang, P.; et al. Weakly solvated electrolyte enables the robust solid electrolyte interface on SiOx anodes for lithium-ion battery. *Chem. Eng. J.* **2024**, *500*, 157028. https://doi.org/10.1016/j.cej.2024.157028.
154. Liu, X.; Shang, J.; Li, J.; et al. Insight into Robust Anion Coordination Behavior of Organic Cathode with Dual Elongated π-Conjugated Motifs. *Angew. Chem. Int. Ed.* **2025**, *64*, e202420160. https://doi.org/10.1002/anie.202420160.